EXPERIMENTAL INVESTIGATION OF CHITOSAN FUNCTIONALIZED GRAPHENE OXIDE BEADS FOR ADSORPTIVE REMOVAL OF METHYLENE BLUE DYE FROM ITS AQUEOUS SOLUTION

A thesis submitted towards the partial fulfilment of the Masters of Engineering degree in Bioprocess Engineering

By

RIDDHI DUTTA

Class Roll No.: 002210303004

Exam Roll No. : M4BPE24004

Registration No. : 163453 of 2022-2023

Under the guidance of

Dr. SASWATA BOSE

&

Dr. MEHABUB RAHAMAN

Department of Chemical Engineering

Jadavpur University

Kolkata – 700032

DECLARATION OF ORIGINALITY AND COMPLIANCE WITH ACADEMIC ETHICS

I hereby declare that this thesis contains a literature survey and original research work by the undersigned candidate, as part of his "***Master of Engineering in Bioprocess Engineering***" study. All information in this document has been obtained and presented following academic rules and ethical conduct.

I also declare that, as required by these rules and conduct, I have fully cited and referenced all materials and results that are not original to the research work.

Name: **RIDDHI DUTTA**

Registration Number: 163453 of 2022-2023

Thesis Title: **"EXPERIMENTAL INVESTIGATION OF CHITOSAN FUNCTIONALIZED GRAPHENE OXIDE BEADS FOR ADSORPTIVE REMOVAL OF METHYLENE BLUE DYE FROM ITS AQUEOUS SOLUTION".**

Signature: Riddhi Dutta

CERTIFICATION

This is to certify that Riddhi Dutta, a final year student in the Master of Engineering examination in the Department of Chemical Engineering, Jadavpur University, bearing Registration No.: 163453 has completed the thesis work entitled **"EXPERIMENTAL INVESTIGATION OF CHITOSAN FUNCTIONALIZED GRAPHENE OXIDE BEADS FOR ADSORPTIVE REMOVAL OF METHYLENE BLUE DYE FROM ITS AQUEOUS SOLUTION"** under the guidance of Dr. Saswata Bose and Dr. Mehabub Rahaman during his course curriculum. This work has not been reported earlier anywhere and can be approved for submission in partial fulfilment of the Master of Engineering in Bioprocess Engineering.

Saswata Bose.

Dr. Saswata Bose
Assistant Professor
Chemical Engg. Dept. JU

Assistant Professor
CHEMICAL ENGINEERING DEPARTMENT
JADAVPUR UNIVERSITY
Kolkata-700 032

Mehabub Rahaman.

Dr. Mehabub Rahaman
Associate Professor
Chemical Engg. Dept. JU

Associate Professor
CHEMICAL ENGINEERING DEPARTMENT
JADAVPUR UNIVERSITY
Kolkata-700 032

Mehabub Rahaman (ofc)

~~Dr. Papita Das~~
Head of the Department
Chemical Engg. Dept. JU

HEAD
CHEMICAL ENGINEERING DEPARTMENT
JADAVPUR UNIVERSITY
Kolkata-700 032

Dipak Laha
02/8/24
Dean
Faculty of Engineering and Technology, JU

DEAN
Faculty of Engineering & Technology
JADAVPUR UNIVERSITY
KOLKATA-700 032

iii

CERTIFICATE OF APPROVAL

This thesis is hereby approved as a creditable study of an engineering subject carried out and presented in a manner satisfactory to warrant its acceptance as a prerequisite to the degree for which it has been submitted. It is understood by this approval that the undersigned don't endorse or approve any statement made, opinion expressed or conclusion drawn therein but approve the thesis only for which it is submitted.

Riddhi Dutta.

Riddhi Dutta

M.E. Exam Roll No. M4BPE24004

Chemical Engg. Dept. JU

ACKNOWLEDGEMENT

Though the following project is individual project work, I would never be successful in smoothly completing my project without help, guidance, assistance and inspiration from a lot of people. At the start of this report, I would like to thank all those persons who have helped me in this endeavour. Without their guidance and help it would not be possible for me to progress and plan about this project.

I would sincerely express my gratitude towards my guide **Dr. Saswata Bose** and **Dr. Mehabub Rahaman** for their valuable guidance and cooperation and for providing me with the opportunity to accomplish the project. Without their guidance and assistance, I would never be able to work successfully in this area. I am greatly thankful to them for guiding me always throughout my project work.

I would like to thank my lab mate who consistently helped me while performing and planning this project.

I would also like to express gratitude to the HOD and all faculties of the Chemical Engineering Department at Jadavpur University.

Thanking You,

Riddhi Dutta

Class Roll No.: 002210303004

Exam Roll No.: M4BPE24004

Registration No.: 163453 of 2022-23

M.E. 2nd Year

ABSTRACT

Unrestricted discharge of dyes in waste water over the years has shown grave concern in the environmental pollution. Researchers have found various adsorbent to check the removal of these menacing dyes affecting the environment. In these paper in order to extract methylene blue (MB) dye from an aqueous medium, the fabrication of Chitosan on Graphene Oxide (CS-GO) composite beads was examined in this work using continuous dropping procedures. Both before and after the MB was adsorbed, the produced beads were characterized using a variety of methods like SEM,FTIR,XRD and DLS. The SEM micrograph demonstrates that Chitosan was successfully deposited on the rough graphene oxide composites. The maximal shift of graphene oxide peak has been detected using XRD data due to broad spectrum Peak of Chitosan. According to the FTIR analysis, as due to red shift in graphene oxide Chitosan composites due to treatment with MB, fewer oxygen-containing functional groups are present. In DLS, there is difference in particle size of GO and CS-GO due to agglomeration of the two compounds. The adsorption processes were found to fit both the Langmuir isotherm and the kinetic Intra diffusion particle models, according to the experimental results. Additionally, the maximum adsorption capacities of 1.633 mg g−1 achieved by the CS-GO beads were equivalent to those of other adsorbents reported in the literature. Our adsorbent's ability to eliminate 91% of the actual sample color in 24 hours is a significant benefit. After 4 cycles of regeneration of the adsorbent, a minor drop in removal efficiency was observed.

TABLE OF CONTENT

DECLARATION OF ORIGINALITY AND COMPLIANCE WITH ACADEMIC ETHICS ii

CERTIFICATION iii

CERTIFICATE OF APPROVAL iv

ACKNOWLEDGEMENT v

ABSTRACT vi

TABLE OF CONTENT vii

LIST OF FIGURES ix

LIST OF TABLES x

LIST OF ABBREVIATIONS xi

CHAPTER 1: INTRODUCTION 1

1.1 OVERVIEW OF DYES IN WASTE WATER 2

1.2 REMOVAL OF DYES FROM WASTEWATER VIA ADSORPTION 4

1.3 REMOVAL OF METHYLENE BLUE DYE USING VARIOUS ADSORBENTS 6

1.4 OBJECTIVES OF PRESENT WORK 17

CHAPTER 2: MATERIALS & METHODS 18

2.1 MATERIALS 19

2.2 METHODS .....

2.2.1 GO Synthesis 19

2.2.2 CS Synthesis 20

2.2.3 CS Functionalized GO beads Synthesis 21

2.2.4 Characterization 22

2.2.5 Calibration Curve data analysis 23

2.2.6 Batch Study 24

CHAPTER 3: RESULTS & DISCUSSION.....25

3.1 CHARACTERIZATION.....

3.1.1 Scanning Electron Microscope Micrograph…….26

3.1.2 X-Ray Diffraction Analysis: 27

3.1.3 Fourier Transform Infrared Ray Analysis: 29

3.1.4 DLS Analysis: 30

3.1.5 Effect of Zero Point Discharge……..31

4.1 EFFECT OF PARAMETERS 32

4.1.1 pH STUDY 32

4.2.2 Effect of Initial Concentration 33

4.2.3 Effect of Adsorbent Dosage.....34

4.2.4 Effect of Temperature.....35

4.3 ADSORPTION THERMODYNAMICS 35

4.4 ADSORPTION KINETICS……41

4.5 ADSORPTION THERMODYNAMICS……44

4.6 REGENERATION STUDY 46

4.7 COMPARISON STUDY TABLE OF VARIOUS ADSORBENT OF PREVIOUS WORK WITH THE PRESENT WORK…….47

CHAPTER 4: CONCLUSION 49

5.1 CONCLUSION 50

REFERENCES 51

LIST OF FIGURES

Figure 1: Chemical Structure of Methylene Blue

Figure 2: Synthesis Process of CS-GO bead Schematically.

Figure 3A and B: Absorbance vs Wavelength and Absorbance vs Concentration graph.

Figure 4A and B: The SEM images of CS-GO beads Untreated.

Figure 5A and B: The SEM images of CS -GO beads treated with MB.

Figure 6: XRD Patterns of CS- GO Beads

Figure 7A and B: FTIR Patterns of CS-GO Beads, MB treated CS-GO Beads

Figure 8A and B: DLS Analysis graphs of GO and GO-CS Beads

Figure 9: Effect of Zero Discharge Point on CS-GO Beads

Figure 10: Effect of Various pH study on Removal percentage.

Figure 11: Removal percentage on Effect of Various initial concentration against Time.

Figure 12: Effect of Various Adsorbent Dosage against Time.

Figure 13: Effect of various temperature against time.

Figure 14 A and B: Linear Langmuir Plot and Temkin isotherm plot of MB. C,D & E : Linear Freundlich, Non Linear Langmuir and Non Linear Freundlich plot of MB.

Figure 15 A, B & C: Pseudo First order,Intra diffusion particle and Pseudo Second order Kinetics plot of MB dye over CS- GO beads .

Figure 16: Thermodynamic Study of MB adsorption of CS-GO.

Figure 17: Regeneration Study of MB- adsorption on CS-GO.

LIST OF TABLES

Table 1: XRD Parameters Table

Table 2: Linear Adsorption isotherm Data Table

Table 3: Non- Linear Adsorption Isotherm Data

Table 4: Adsorption Kinetics Data

Table 5: Adsorption Thermodynamics Data

LIST OF ABBREVIATIONS

MB = Methylene Blue

GO = Graphene Oxide

CS-GO = Chitosan- Graphene Oxide composite

CS = Chitosan

UV- Vis = UV-Vis Spectroscopy

SEM = Scanning Electron Microscope

TEM= Transmission Electron Microscope

XRD = X-Ray Diffraction

FTIR = Fourier Transform Infrared Ray

DLS = Dynamic Light Scattering

CHAPTER -1

INTRODUCTION

1.1 OVERVIEW OF DYES IN WASTE WATER

Dyes are chemical compounds that bind to substrates or textiles, imparting color. Most dyes are complex organic molecules engineered to withstand various factors, including detergent action. Synthetic dyes find extensive applications in advanced technological fields such as textiles, paper, leather tanning, food processing, plastics, cosmetics, rubber, printing, and dye manufacturing. They are also utilized in groundwater tracing, determining the specific surface area of activated sludge, and wastewater treatment. The environmental impact of dye discharges is significant due to their persistent nature, leading to long-term pollution in aquatic ecosystems. This pollution results in undesirable coloration of water bodies, reducing sunlight penetration and inhibiting photochemical and biological processes essential for aquatic life.[1] Current data indicates the existence of over 100,000 commercial dyes, with an annual production exceeding 700,000tonnes. The global textile industry alone consumes over 10,000tonnes of dyes annually, and approximately 100tonnes are discharged into water streams each year. Despite the lack of precise data on dye discharge from various environmental processes, the substantial release of synthetic dyes poses a challenge to environmental scientists.[2] To mitigate the environmental impact, several methods are employed to remove dyes from wastewater. These methods include adsorption, coagulation, advanced oxidation, and membrane separation. Researchers have also enhanced the adsorption capacity of raw biomass adsorbents through various physical and chemical treatments. Adsorption, in particular, is a widely studied method for dye removal due to its efficiency and cost-effectiveness.[3] This review highlights the current advancements in adsorption techniques for dye removal from aqueous solutions. It focuses on the development and application of commercial activated carbon and sustainable, low-cost alternative adsorbents derived from agricultural solid waste, industrial solid waste, agricultural by-products, biomass-based activated carbon, and various natural materials.[4] The review critically analyzes the effectiveness of these adsorbents under different physicochemical parameters. Factors such as pH, temperature, contact time, and adsorbent dosage are examined to determine their impact on adsorption efficiency. Additionally, the review compares the adsorption capacities of different adsorbents, providing a comprehensive overview of their performance. Commercial activated carbon is widely recognized for its high adsorption capacity and effectiveness in dye removal. However, its high cost has led to the exploration of alternative adsorbents that are both sustainable and cost-effective. Agricultural solid waste, industrial solid waste, and agricultural by-products

are abundant and inexpensive materials that have shown promising results as adsorbents for dye removal.[3] Biomass-based activated carbon, derived from sources such as coconut shells, rice husks, and sawdust, is another viable alternative. These materials undergo physical or chemical treatments to enhance their adsorption properties, making them effective in removing dyes from wastewater. Furthermore, natural materials such as clay, zeolites, and chitosan have been investigated for their adsorption potential. These materials are readily available, environmentally friendly, and possess good adsorption properties. The review discusses the advantages and limitations of each type of adsorbent, providing insights into their practical applications. In conclusion, the review presents a comprehensive overview of the current advancements in adsorption techniques for dye removal from aqueous solutions.[6] It emphasizes the development of sustainable, low-cost adsorbents derived from various sources and critically analyzes their effectiveness under different physicochemical conditions. By exploring alternative adsorbents, researchers aim to provide environmentally friendly solutions for dye removal, addressing the challenges posed by synthetic dye pollution in water bodies.

Several treatments, such as coagulation, flocculation, biodegradation, membrane filtration, reverse osmosis, and adsorption, have been implemented to separate dye moieties from aqueous solutions. Of these methods, adsorption-based processes are regarded as the most efficient due to their ability to continuously treat large volumes of high-strength wastewater in a simple and cost-effective manner without using organic solvents. Recent research has focused on the use of nanomaterials as adsorbents because they can be synthesized cost-effectively and require only small quantities to effectively remove pollutants from effluents. Among various nanomaterials, graphene oxide (GO) has gained significant attention due to its non-toxic nature, ease of synthesis, prominent and uniform structures, and high stability. Single-layered GO sheets dispersed in an aqueous medium provide maximum surface area for adsorption, though retrieving these sheets from water for reuse can be inconvenient. To address this issue, studies have explored using chitosan (Cs), a biopolymer, as a crosslinking agent for GO. This approach prevents aggregation, enhances the available surface area for adsorption, and reduces both the required adsorbent dosage and contact duration. The combination of GO and CS offers a promising solution for efficient and cost-effective dye removal from wastewater.[6]

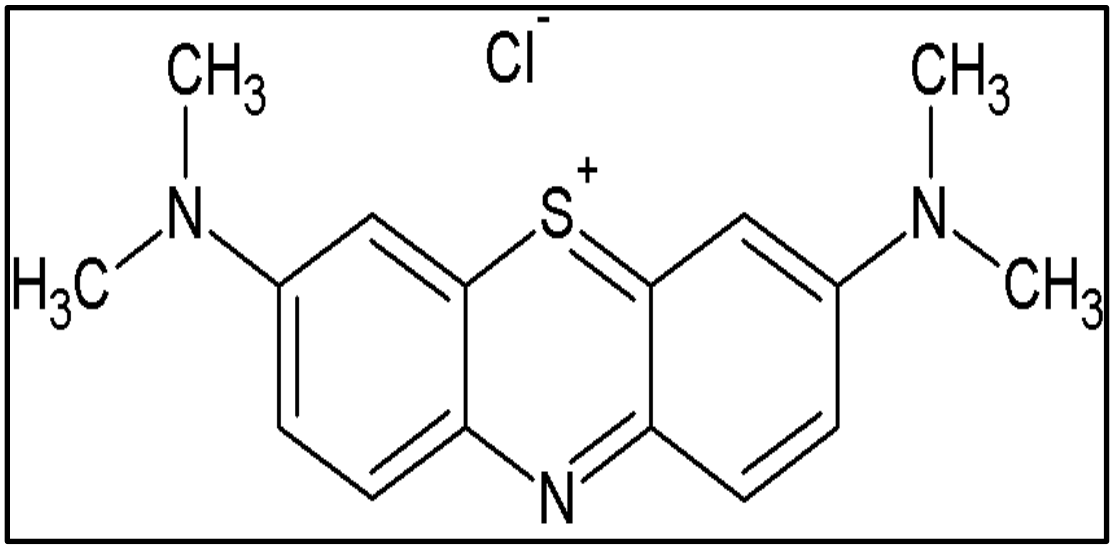


Figure 1: Structure of Methylene Blue

1.2 REMOVAL OF DYES FROM WASTEWATER VIA ADSORPTION

In a Liquid or a solid substance, a molecule present within bulk of substance being attracted uniformly from all sides by the neighboring molecules. Hence, there is no net force acting on the molecule or there are no unbalanced forces of the molecule. On the other hand molecules present On the surface is not attracted to the other molecules from all sides because there are no neighboring molecules above the surface. Hence, it possesses some unbalanced or residual forces. The accumulation of molecular species (gas or liquid) at the surface of solid or liquid rather than in a bulk , is referred to as adsorption. This causes increase in concentration of other Molecule species near to the surface. [7]. The process of adsorption consists of three phases. The adsorbate molecules initially diffuse into the solid-fluid external interphase from the bulk phase. We call this "film diffusion." The molecules spread into the pores in the second process, which is referred to as particle diffusion.[9] The adsorption takes place on the adsorbent surface during the third phase. Adsorption isotherms describe the relationship between the adsorbate in the liquid phase and the adsorbate adsorbed on the adsorbent surface at equilibrium at a constant temperature. [10]. Numerous adsorbents have been employed in wastewater treatment over time. Alumina, zeolite, silica gel, activated carbon, and others are a few of them. The cost of activated carbon is relatively high. Reusing activated carbon requires treating it with a solvent, which is also highly expensive. Alternative techniques, such as thermal and homogeneous advanced oxidation (UV/H2O2 and H2O2/O3), have been studied but are hardly ever used. Zeolite also has certain

drawbacks, such as its extreme sensitivity to deactivation by steric obstruction or irreversible adsorption of heavy secondary products, and its inability to use its microporosity for the synthesis of large molecules. Due to the high relative pressure needed for adsorption, silica gel's primary drawback is its limited water exchange and low adsorption capacity.[11] One of the latest generation of nanoparticles that can be utilized as an adsorbent is graphene oxide, a 3D sheet of carbon atoms organized in a hexagonal lattice. Its high surface area to mass ratio results in a large number of adsorption sites along with a uniform pore distribution. There is also a great deal of surface resistance. Owing to its hexagonal lattice structure, graphene produces a cloud of delocalized electrons that engage in π-π stacking interactions with other molecules. Poor water dispersibility of graphene is its primary disadvantage when it comes to water treatment. However, surface functionalization provides a solution to the issue of low dispersibility, could be
With metal oxide, organic compound and rest.

Researchers found that Chitosan (CS), a natural biopolymer, is a promising adsorbent material derived from natural resources and has gained significant attention due to its advantageous properties. Its chemical structure contains several active groups, such as amino (-NH2) and hydroxyl (-OH) groups, which act as coordination sites for various pollutants, making it an efficient adsorbent for wastewater treatment. Recent studies have focused on modifying chitosan to enhance its efficiency in removing dyes and other pollutants from wastewater. One approach involves modifying CS with carboxymethyl groups to create a novel cross-linked O-CM-chitosan hydrogel adsorbent for MB dye removal. Other innovative adsorbent materials include activated carbon-CS microbeads and a sponge material made of karaya gum and CS, both designed to adsorb MB dye from wastewater. Additionally, polyacrylamide (PAAM)/CS adsorbents have been explored as low-cost, eco-friendly bio-adsorbents for MB dye decolorization. Graphene oxide (GO) is currently used as an adsorbent for various pollutants in wastewater due to its numerous oxygen-containing functional groups. To enhance CS's adsorption capacity for cationic dyes, GO is introduced onto CS to incorporate additional carboxylic groups as active anionic sites, improving its dye adsorption capabilities from aqueous media.

1.3 REMOVAL OF METHYLENE BLUE DYE USING VARIOUS ADSORBENTS

Ghaedi M et al (2014) This study assessed the effectiveness of Au-NP-AC, or gold nanoparticles loaded on activated carbon, in removing BTB(Bromothymol Blue) and Methylene Blue (MB) from aqueous solutions. The effects of a number of variables on dye adsorption were investigated, including temperature, Au-NP-AC amount, initial dye concentration, and solution pH. The Langmuir, Freundlich, Temkin, Dubinin–Radushkevich and Harkins–Jura isotherm models were used to examine equilibrium data. The equilibrium results fit well by the Langmuir model, which had adsorption capacities of 95.24 mg/g for BTB and 40.65 mg/g for MB. The adsorption of both dyes on the adsorbent surface was found to follow a pseudo-second-order model, according to kinetic analysis. [27]

Hoa N.V et al (2021) This study assessed Highly porous hydroxyapatite/Graphene Oxide/Chitosan beads as an effective adsorbent for dyes and heavy metals ion removal. Effects of a number of variables on dye adsorption were investigated, including temperature, adsorbate amount, initial dye concentration, and solution pH. The Langmuir, Freundlich, Dubinin–Radushkevich, and Temkin isotherm models were used to examine equilibrium data. The equilibrium results fit well by the Langmuir model, which had adsorption capacity of 99.00 mg/g for MB. The adsorption of dye on the adsorbent surface was found to follow a pseudo-second-order model, according to kinetic analysis.[41]

Sammaar AL et al(2022) In This study there was shown Chitosan and Alginate based hydrogel beads for the adsorption of Anionic and Cationic dyes from Water . The results show that Hydrogels synthesized with greater yield showed great removal (more than 90%).Effects of a number of variables on dye adsorption were investigated, including temperature, adsorbate amount, initial dye concentration, and solution pH. The Langmuir, Freundlich, Dubinin–Radushkevich, and Temkin isotherm models were used to examine equilibrium data. The equilibrium results fit well by the Langmuir model, which had adsorption capacity of 15.00 mg/g for MB. The adsorption of MB was found higher at pH 8.5. [20]

Wang, Z et al (2020) This study was carried out about Preparation of Chitosan/ Polyacrylamide/Graphene oxide composite Membranes and Study of their Methylene Blue Adsorption properties. Effects of a number of variables on dye adsorption were investigated, including temperature, adsorbate amount, initial dye concentration, and pH of the solution.Removal efficiency after three cycles was 90.18%. The Langmuir, Freundlich, Dubinin–Radushkevich and Temkin isotherm models were used to examine equilibrium data. The equilibrium results fit well by the Langmuir model, with maximum monolayer formation which had adsorption capacity of 510.2 mg/g for MB. Kinetic researchers disclosed that The adsorbent surface was found to follow a pseudo-second-order model, according to kinetic analysis. Thermodynamic researches reveal that the enthalpy change(ΔH) as well as Gibbs Free energy(ΔG)was negative.[19]

Marotta, A(2020) This study assessed Chitosan/Zeolite composite Aerogels for a fast and effective removal of Both Anionic dyes and Cationic dyes from Water. Batch studies of variables on dye adsorption were investigated, including temperature, adsorbate amount, initial dye concentration, and solution pH. The Langmuir, Freundlich and Temkin isotherm models were used to examine equilibrium data. The equilibrium results fit well by the Langmuir model, which had adsorption capacity of 108 mg/g for MB. The adsorption of MB dyes on the adsorbent surface was found to follow a pseudo-First-order(PFO) model, according to kinetic analysis. 90% of the sample was absorbed at 24 hours.[34]

Dindorkar .S et al (2021) This study assessed Adsorptive removal of methylene blue dye from aqueous streams using Photocatalytic CuBTC/ZnO Chitosan composites . Effects of a number of variables on dye adsorption were investigated, including temperature, adsorbate amount, initial dye concentration, and solution pH was observed. The Langmuir, Freundlich, Dubinin–Radushkevich, and Temkin isotherm models were used to examine equilibrium data. The equilibrium results fit well by the Langmuir model, indicating adsorption was monolayer and Chemical in nature. The adsorption of dye on the adsorbent surface was found to follow a pseudo-second-order model, according to kinetic analysis.Maximum Adsorption capacity of 50.07 mg/g for MB. It has a removal efficiency of 98.75% of MB by the composite.[24]

Siregar P.M.S et al(2016) This study assessed Mg/Al- Chitosan as a selective adsorbent in the removal of Methylene Blue from Aqueous Solutions. Batch studies of variables on dye adsorption were investigated, including temperature, adsorbate amount, initial dye concentration, and solution pH. It took 90 mins for adsorption to reach equilibrium. The Langmuir, Freundlich and Temkin isotherm models were used to examine equilibrium data. The equilibrium results fit well with the Langmuir model, where adsorption occurs chemically(monolayer) which has an adsorption capacity of 108.696 mg/g for MB. Regeneration study shows that Mg/Al Chitosan is an adsorbent that can be used repeatedly with stable adsorption effectiveness until the fifth cycle.[44]

Sabzevari (2018) Graphene oxide (GO) was cross-linked with chitosan to yield a composite (GO-LCTS) with variable morphology, enhanced surface area, and notably high methylene blue (MB) adsorption capacity. The materials were structurally characterized using thermogravimetric analysis and spectroscopic methods (X-ray diffraction, Fourier transform infrared spectroscopy, Raman spectroscopy, and 13C solid-state NMR) to support that cross-linking occurs between the amine groups of chitosan and the −COOH groups of GO. Equilibrium swelling studies provide support for the enhanced structural stability of GO-cross-linked materials over the synthetic precursors. Scanning electron microscopy studies reveal the enhanced surface area and variable morphology of the cross-linked GO materials, along with equilibrium and kinetic uptake results with MB dye in aqueous media. The Adsorption capacity with MB reveals variation for Qm, where GO-LCTS (402.6 mg/g) and GO (286.9 mg g−1). The kinetic uptake profiles of MB follow a pseudo-second-order trend, where the GO composite shows more rapid uptake over GO. This study reveals that the sorption properties of GO are markedly improved upon formation of a GO−chitosan composite. It fits the best in Langmuir isotherm model.[38]

Hamid Abd El et al(2018) This study was carried out about Graphene oxide: Follow the oxidation mechanism and its application in water treatment. Effects of a number of variables on dye

adsorption were investigated, including temperature, adsorbate amount, initial dye concentration, and pH of the solution.. The Langmuir, Freundlich, Dubinin–Radushkevich, and Temkin isotherm models were used to examine equilibrium data. The equilibrium results fit well with the Langmuir model, with maximum monolayer formation which had adsorption capacity of 357.14mg/g for MB. Kinetic researchers disclosed that The adsorbent surface was found to follow a pseudo-second-order model(PSO), according to kinetic analysis. Four consecutive cycles were Performed for regeneration study. [45].

Arunachalam, K.D(2021) This study was assessed on the Bio adsorption of Methylene Blue dye using Chitosan extracted from *Ferrero penaeus indicus* Shrimp shell waste. Removal efficiency was 93.23%. The maximum amount of dye adsorption was obtained at a minimum dose of 4g. Chitosan was found to be better absorbent . The species has its own bio-remediation for MB in sample water. It took 4 hours for the equilibrium to attain.[21]

Martis, L.J et al(2022) This study used a variety of analytical approaches to successfully construct and characterize silk fibroin/graphene oxide (SF/GO) blend films for Methylene Blue adsorption.The integration of GO with SF was verified by UV-visible spectroscopy (UV-Vis), and pictures from scanning electron microscopy (SEM) showed that GO was uniformly distributed throughout the SF matrix, increasing the roughness of the film. In comparison to native SF, the SF/GO films showed improved thermal stability, according to thermogravimetric analysis (TGA). As novel adsorbents for methylene blue (MB), Naive SF and SF/GO blend films were assessed; they achieved removal efficiencies of 86% and 96%, respectively. A thorough investigation was conducted into the effects of pH, contact time, concentration, and adsorbent dosage on dye adsorption. The pseudo-second-order model was supported by the adsorption kinetics, which showed strong linear fit correlations followed by the Freundlich isotherm model. Maximum Adsorption Capacity is 381.67 mg/g for SF/GO and 235. 84 mg/g for SF. [35]

Fu,J et al(2015) This study assessed adsorption of methylene blue by high efficiency adsorbent polydopamine spheres. UV-visible spectroscopy (UV-Vis), field emission scanning electron

microscopy (FE-SEM) showed that microspheres were uniformly distributed , increasing the roughness of the material). As novel adsorbents for methylene blue (MB), Polydopamine microspheres blend were assessed. A thorough investigation was conducted into the effects of pH, contact time, concentration, and adsorbent dosage on dye adsorption. The pseudo-second-order model was supported by the adsorption kinetics, following the adsorption behavior. From all the isotherm studies conducted, equilibrium data best fitted the langmuir isotherm, having an adsorption capacity of 90.07 mg/g. Thermodynamic analysis showed that the adsorption was endothermic and spontaneous. [26]

Munir, M et al (2020) This study assessed the effective adsorptive removal of Methylene Blue from water by didodecyldimethyl ammonium Bromide-modified Brown clay. Effects of a number of variables on dye adsorption were investigated, including temperature, adsorbate amount, initial dye concentration, and solution pH. The Langmuir, Freundlich and Temkin isotherm models were used to examine equilibrium data. The equilibrium results fit well with the Langmuir model, which had adsorption capacity of 164 mg/g for MB. The adsorption of dye on the adsorbent surface was found to follow a pseudo-second-order model, according to kinetic analysis. It showed a maximum removal efficiency of 98% after 24 hours. [25]

Abd- Elhamid, A.I et al (2019) In this paper the study of activated charcoal for purification of water from colored organic pollutants. Effects of a number of variables on dye adsorption were investigated, including temperature, adsorbate amount, initial dye concentration, and solution pH. Removal percentage of MB dye was around 98%. The Langmuir, Freundlich, Dubinin–Radushkevich, and Temkin isotherm models were used to examine equilibrium data. The Langmuir model was the most fit to experimental adsorption with maximum adsorption capacity of 114.42 mg/g . The adsorption of dye on the adsorbent surface was found to follow a pseudo-second-order model, according to kinetic analysis and with best coefficients investigated for the adsorption process. Five cycles were performed to check the regeneration efficiency.[46]

Al. Nayl ,Ad El Aziz et al(2022) In this study, Preparation of graphene oxide-chitosan composite beads as an effective adsorbent to remove Cationic dye. From aqueous media.
The beads prepared was characterized by TGA(Thermogravimetric Analysis), FTIR, SEM For understanding better beads. The experimental results showed that the adsorption process fits Langmuir isotherm model with maximum adsorption capacity of 23.26 mg/g. The model followed Pseudo second order according to kinetic analysis The adsorbent could remove 82.1% of the color sample within 135 mins.[36]

Yang et al(2011) In this work, graphene oxide- composite are made in order to effectively adsorb MB from aqueous solutions. XRD(X-Ray diffraction), Fourier-transform infrared spectroscopy (FTIR), and scanning electron microscopy (SEM) were used to analyze .. Based on experimental data, the maximum adsorption capacity of 714mg/g was found, and the adsorption process followed the Langmuir isotherm model. At initial MB concentration lower than 250 mg/l the removal efficiency is higher than 99%. Regeneration was followed for 5 cycles.[47]

Rahmi et al(2019) The Study was assessed that Magnetic chitosan nanocomposite beads crosslinked with H2SO4 were created and used as adsorbents to remove methylene blue. The beads of nanocomposite were made with varying concentrations of H2SO4 and Fe3O4.
XRD and SEM studies were used to prepare and validate the nanosized Fe3O4 crystallite. H2SO4 crosslinked magnetic chitosan nanocomposite beads were created using the Fe3O4 crystallite, and FTIR, XRD, and SEM analysis verified the beads production. Adsorption tests were carried out with various contact durations, pH levels, and starting methylene blue concentrations. After 25 minutes of contact time, the equilibrium of methylene blue adsorption by H2SO4 crosslinked magnetic chitosan nanocomposite beads was achieved with adsorption capacity of 20.408 mg/g. Adsorption isotherm best fits on Langmuir model and follows pseudo second order kinetics model as a part of kinetic analysis.[37]

Fawwaz Al et al (2016) This study assessed Decolorization of Methylene Blue and Malachite green by immobilized *Desmodesmus* sp. Effects of a number of variables on dye adsorption were investigated, including temperature, adsorbate amount, initial dye concentration, and solution pH, Contact time. The Langmuir, Freundlich and Temkin isotherm models were used to examine equilibrium data. The equilibrium results fit well with the Langmuir model, which had adsorption capacity of 20 mg/g for MB.. It showed a maximum removal efficiency of 98.6% and the decolorization ability of immobilized *Desmodesmus* sp. Against both the dyes were observed.[18]

Sen et al(2011) This study assessed the Equilibrium, Kinetics and Mechanism of Removal of Methylene Blue from Aqueous solution by adsorption onto pine cone biomass and *pinus radiata*. Effects of a number of variables on dye adsorption were investigated, including temperature, adsorbate amount, initial dye concentration, and solution pH. The Langmuir, Freundlich and Temkin isotherm models were used to examine equilibrium data. The equilibrium results fit well with the Langmuir model, which had adsorption capacity of 109.89mg/g for MB. Maximum monolayer adsorption capacity was observed at 30 degree Celsius. The adsorption of dye on the adsorbent surface was found to follow a pseudo-second-order model, according to kinetic analysis. Thermodynamic nature indicates that the system is Spontaneous, Exothermic and Physical process in nature.[48]

Wang et al(2019) This study was about the self-assembled polyelectrolyte based on composite hydrogels with enhanced stretchable and adsorption performances . Effects of a number of variables on dye adsorption were investigated, including temperature, adsorbate amount, initial dye concentration, and solution pH. The Langmuir, Freundlich and Temkin isotherm models were used to examine equilibrium data. The equilibrium results fit well with the Langmuir model, which had adsorption capacity of 6.03 mg/g for MB. The adsorption of dye on the adsorbent surface was found to follow a pseudo-First Order model, according to kinetic analysis.[42]

Liu et al(2019) This study assessed the rapid synthesis of silsesquioxane-based disulfide -linked polymer for selective removal of cationic dyes from aqueous solution. Effects of a number of variables on dye adsorption were investigated, including temperature, adsorbate amount, initial dye concentration, and solution pH. The Langmuir, Freundlich and Temkin isotherm models were used to examine equilibrium data. The equilibrium results fit well with the Langmuir model, which had adsorption capacity of 12.94mg/g for MB. The adsorption of dye on the adsorbent surface was found to follow a pseudo-second-order model, according to kinetic analysis. It showed a maximum removal efficiency of 95% after 24 hours. In this study we find 5 runs of the regeneration cycle of adsorption was observed.[32]

Nurus et al (2022) This study is about the preparation of Chitosan/iron oxide-based biocomposite and its application as a potential adsorbent for the removal of Methylene Blue from aqueous solution. Effects of a number of variables on dye adsorption were investigated, including temperature, adsorbate amount, initial dye concentration, and solution pH. The Langmuir, Freundlich and Temkin isotherm models were used to examine equilibrium data. The equilibrium results fit well with the Langmuir model, which had adsorption capacity of 16 mg/g for MB. The adsorption of dye on the adsorbent surface was found to follow a pseudo-second-order model, according to kinetic analysis. It showed a maximum removal efficiency of 98% after 24 hours. [39]

Deng et al (2020) This study assessed the Honeycomb-like structure-tunable Chitosan based porous Carbon microspheres for Methylene Blue efficient removal. Effects of a number of variables on dye adsorption were investigated, including temperature, adsorbate amount, initial dye concentration, and solution pH. The Langmuir, Freundlich and Temkin isotherm models were used to examine equilibrium data. The equilibrium results fit well with the Langmuir model, which had adsorption capacity of 1599.03 mg/g for MB. Various Characterization done for microspheres like FT-IR, BET, SEM, TEM . Specific Surface area was observed of 2463.9 m^2/g The adsorption of dye on the adsorbent surface was found to follow a pseudo-second-order model, according to kinetic analysis. After 5 Cycles of regeneration the (CPCM) remained 80% . A slight adsorption

efficiency loss happened after the 6th cycle, which might be attributed to the surface and internal dense porous structure of CPCM-800. [23]

Popoola (2019) This study assessed the Characterization and adsorptive behavior of snail-shell-rice husk(SS-RH) calcined particles(CP'S) towards cationic dye . Effects of a number of variables on dye adsorption were investigated, including temperature, adsorbate amount, initial dye concentration, and solution pH. The Langmuir, Freundlich and Temkin isotherm models were used to examine equilibrium data. The equilibrium results fit well with the Langmuir model, which had adsorption capacity of 129.870 mg/g for MB. The adsorption of dye on the adsorbent surface was found to follow a pseudo-second-order model, according to kinetic analysis. [40]

Gurses et al(2006) The adsorption kinetics of a cationic dye, methylene blue, onto clay from aqueous solution were examined in this work in relation to the sorbent dosage, temperature, pH, mixing rate, and initial dye concentration. Zeta potentials, the conductivities of clay suspensions at different pH (1–11), and the cation exchange capacity (CEC) were investigated in order to gain a detailed understanding of the adsorption mechanism. BET surface area measured. The outcomes demonstrated that the adsorption reached equilibrium in a single hour with adsorption capacity of 58.2 mg/g . It was discovered that as the temperature drops and as the sorbent dosage and initial dye concentration rise, so does the amount of methylene blue adsorbed . The adsorption kinetics of methylene blue have been investigated in terms of pseudo-first-order, pseudo-second-order, and intraparticle diffusion processes. It was discovered that the pseudo-second-order mechanism predominates and that more than one step appears to be in charge of controlling the dye adsorption process' overall rate.[30]

Gunathilake et al (2023) The removal of methylene blue (MB) from aqueous solutions is investigated utilizing raw laterite soil as an inexpensive adsorbent. Surface area and physio-chemical characteristics were ascertained. The effects of variables on MB adsorption by raw laterite were investigated, including contact time, laterite dosage, pH, and ionic salts. The findings

demonstrated that, at pH levels above 10, after 60 minutes of contact time, and with an adsorbent (raw Laterite) dose of 1.00 g in 100mL of dye solution, the greatest removal effectiveness of MB adsorption was observed. It was observed that the pseudo-second order kinetic model fits the experimental data. The experimental adsorption data fit best by the Freundlich adsorption isotherm model .The estimated adsorption capacity of raw laterite, based on the Freundlich isotherm model, was 2.949 mg/g. According to desorption tests using various solvents, the adsorbent could effectively retain MB up to 33.89%. Thus, it may be concluded that MB can be effectively removed from aqueous solutions using raw laterite soil.[29]

Liu et al(2020) The Study was assessed about HKUST-1 modified ultra stability cellulose/Chitosan Composite aerogel for highly efficient removal of Methylene Blue. The effects of variables on MB adsorption by HKUST-1 component aerogel were investigated, including contact time, laterite dosage, pH, and ionic salts. BET was performed having a surface area of 457.75 m^2/g. It was observed that The pseudo-First order kinetic model fits the experimental data. The experimental adsorption data fit best by the Langmuir adsorption isotherm model .The estimated adsorption capacity of MB , based on the Freundlich isotherm model, was 526.3 mg/g. It has a good recyclability capability.[33]

Almeida (2008) The Study was assessed on Removal of Methylene Blue from Colored effluents by adsorption on montmorillonite clay. The effects of variables on MB adsorption by montmorillonite clay were investigated, including contact time, laterite dosage, pH, and initial concentrations. It was observed.the pseudo-second order kinetic model fits the experimental data. The experimental adsorption data fit best by the Langmuir adsorption isotherm equation .The estimated adsorption capacity of Montmorillonite clay , based on the Langmuir isotherm model, was 4.5 mg/g. Thermodynamic studies were carried out , parameters show that adsorption is an endothermic, yet Spontaneous process. [19]

Ghosh et al (2001) The Study was assessed on Adsorption of Methylene Blue on Kaolinite.

The effects of variables on MB adsorption by montmorillonite clay were investigated, including contact time, laterite dosage, pH, and initial concentrations. . The experimental adsorption data fit best by the Langmuir adsorption isotherm equation.It has an adsorption capacity of 20.49 mg/g. It has the highest capacity for NaOH treated pure Kaolin and lowest for Calcined Samples.
Thermodynamic Studies were conducted and the standard enthalpy change(ΔH) denotes the process is endothermic in nature. The value of (ΔS) is Large and indicates increase in adsorption.[28]

Atun et al(2003) The study was assessed on the Adsorptive removal of Methylene Blue from Colored effluents on Fuller's Earth. The effect of Variables Like pH, Dosage, Initial concentration, Ionic Charges were observed. The adsorption data was best fit by Langmuir isotherm having a adsorption capacity of 79.02 mg/g. Thermodynamic parameters like standard Enthalpy, Entropy were calculated. Values of ΔG are negative, indicating favorable adsorption.
Since ΔH is close to Zero and ΔS is positive,the adsorption mechanism is entropy controlled process.[22]

1.4 OBJECTIVES OF PRESENT WORK :-

There are no certain rules and regulations to impose on dye removal processes used nowadays that are more costly and skilled labors are required which is not affordable for all scales of industries (ex: Textiles, Pulp and paper etc.). That is the main reason for the work is preparation of an adsorbent which is highly efficient, easy to recover, offer physical Characteristics like significant large surface area and pore size and selective dyes.

The objectives of the work are as follows:-

a. Procurement of graphite powder and preparation of graphene oxide (GO) by the modified Hummer's method.
b. Preparation of Chitosan Functionalized Graphene Oxide (CS-GO) nanocomposite beads to carry out investigative analysis of removal of MB dye.
c. Examination of the effects of various parameters including pH range, contact time, initial adsorbate (dye) concentration, adsorbent dosage, and temperature.
d. Analysis of morphology and microstructure using scanning electron microscopy (SEM), metal composition through X-ray diffraction (XRD), and the presence of MB spectrophotometric peaks by UV-Visible spectroscopy. Functional group presence confirmed by Fourier-transform infrared spectroscopy (FTIR).
e. Analysis of adsorption isotherms including linear and nonlinear Langmuir and Freundlich isotherms, and the linear Temkin isotherm.
f. Study of adsorption kinetics using pseudo-first-order, pseudo-second-order models, and intra-particle diffusion.
g. Thermodynamic analysis to determine enthalpy change, Free energy, spontaneity, and system randomness.
h. Regeneration study to assess the reusability efficiency of CS-GO.

CHAPTER -2

MATERIALS AND METHODS

2.1 MATERIALS

All chemical reagents were of analytical grade and were further used without purification. Fine Graphite powder (98%) and Hydrogen peroxide (H_2O_2) (About 30%) were obtained from LOBA chemie, India. Potassium Permanganate ($KmnO_4$) and Concentrated Sulfuric Acid(H_2SO_4), Hydrochloric Acid (HCl) (About 37% for analysis), Sodium Chloride (NaCl) and Sodium hydroxide (NaOH)pellets were procured from Merck, India. Glacial Acetic Acid (CH_3COOH) (99%) and Methylene Blue Strain (Adsorption Maxima= 663-664nm) were purchased from Merck, India. Distilled Water(H20) was used in every batch experiment for washing.

2.2 METHODS

2.2.1 GO Synthesis

Graphene oxide (GO) was synthesized from graphite flakes using a modified Hummer's method, a widely recognized procedure for producing GO. The synthesis process began by placing 4 grams of graphite into a 500 mL flask. To this, 100 mL of concentrated sulfuric acid (H_2SO_4) was added while the flask was kept in an ice bath to maintain a low temperature and control the reaction rate. Following this, 2 grams of sodium nitrate ($NaNo_3$) were added to the mixture, which was then stirred continuously for 4 hours to ensure thorough mixing and reaction.

Next, 12 grams of potassium permanganate ($KmnO_4$) were slowly added to the mixture, which was stirred for an additional 2 hours. The gradual addition of $KmnO_4$ is critical to prevent a rapid reaction that could lead to overheating. After the initial reaction period, the ice bath was removed, and the reaction mixture was heated to 35°C for 30 minutes to facilitate the oxidation process. To further process the mixture, 240 mL of distilled water was added slowly, which caused the temperature to rise to 90°C. This temperature was maintained while the mixture was stirred for another 30 minutes to ensure complete oxidation. To terminate the reaction, 160 mL of distilled water and 30% hydrogen peroxide (H_2O_2) were added. The addition of H_2O_2 is essential as it reacts with any remaining $KmnO_4$ and manganese dioxide (MnO_2), effectively halting the oxidation process and ensuring the safety of the procedure. The resulting solution was stirred overnight to allow the reaction to reach completion and then purified through multiple washings. The mixture was washed with distilled water, 30% hydrochloric acid (HCl), and ethanol until the pH reached

neutrality (pH 7), indicating the removal of acidic by-products and impurities. Finally, the solid GO was collected and vacuum-dried at 40°C to produce dried GO powder. This method ensures the production of high-quality GO with a consistent structure and desirable properties for various applications in research and industry. The high oxidation level achieved through this process imparts GO with a large number of oxygen-containing functional groups, enhancing its solubility and reactivity in aqueous solutions. These properties make GO a versatile material for applications in areas such as water treatment, energy storage, and composite material. The detailed purification steps further guarantee that the final product is free from impurities, ensuring its reliability and efficiency in practical applications[14].

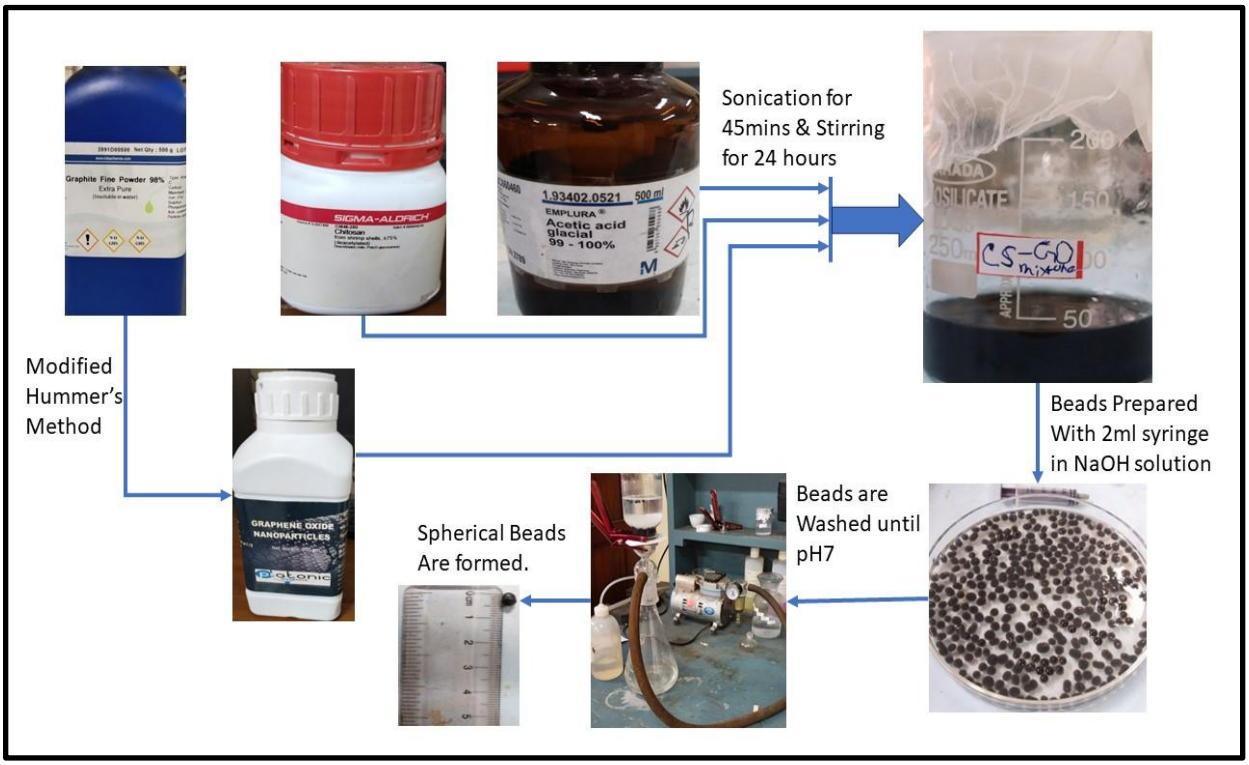
2.2.2 CS Synthesis

Chitosan extraction from prawn shells involved a methodical series of steps to maximize efficiency and yield. Initially, frozen prawn shells underwent washing with boiled water and drying at 60°C to remove impurities and reduce moisture content. The dried shells were then crushed and treated with 5% NaOH, followed by refluxing at 60°C for 2 hours to dissolve organic matter and enhance purity. Subsequent acetone treatment at 25°C for 24 hours effectively removed residual colors and pigments. To dissolve calcium carbonate ($CaCO_3$), the shells were exposed to 0.5% or 1% HCl solution for 24 hours at 25°C. Deacetylation of purified chitin to chitosan was achieved using NaOH solution at elevated temperature and concentration, followed by thorough washing with distilled water to eliminate residues. The resulting chitosan was dried in a vacuum oven at 60°C, yielding a pure product suitable for various applications. These streamlined biological processes not only ensure high-quality chitosan production but also optimize resource efficiency and reduce production costs compared to conventional chemical methods, highlighting the sustainability and practicality of utilizing prawn shell waste in biopolymer [15].

2.2.3 CS Functionalized GO beads Synthesis

The synthesis of CS-GO beads involved a systematic procedure starting with the dispersion of Chitosan (4 g) and Graphene Oxide (GO, 0.3 g) in 100 mL of aqueous acetic acid solution (3%, v/v). The mixture underwent ultrasonication for 1 hour followed by overnight stirring for 24 hours to ensure thorough dispersion and interaction between Chitosan and GO. Subsequently, the prepared mixture was slowly injected into a 300 mL NaOH solution (30%, w/v) using 10-mL

syringes. This step facilitated the formation of spherical CS-GO beads as the Chitosan and GO components reacted and precipitated in the alkaline environment. To remove any residual sodium hydroxide and achieve a neutral pH, the beads underwent several washes with distilled water. This washing process is crucial to ensure the biocompatibility and stability of the CS-GO beads for further applications. After washing, the CS-GO beads were air-dried to remove excess moisture and to stabilize their structure for subsequent use. This drying step is essential to maintain the integrity and functionality of the beads. Overall, the synthesis of CS-GO beads involves controlled dispersion, interaction in an acidic medium, precipitation in an alkaline environment, thorough washing to remove impurities, and careful drying to preserve structural integrity. [16]



The Synthesis process of CS- GO beads formation Schematically:(Fig 2)

2.2.4 Characterization

The adsorbent CS-GO underwent comprehensive characterization using various analytical techniques to elucidate its properties and suitability for applications. UV-VIS spectroscopy was performed with a PerkinElmer L650 UV-Vis spectrophotometer after stirring CS-GO in distilled water for 24 hours to ensure a uniform suspension. Spectral analysis, conducted with a scanning interval of 1 nm and a rate of 2000 nm/min, provided insights into the adsorbent's optical properties and potential for light absorption in different wavelengths. X-ray diffraction (XRD) analysis was carried out using a Rigaku Ultima III X-ray diffractometer at 1.54 Å wavelength, 40 kV voltage, and 30 mA current. This technique generated a diffraction pattern, revealing the crystalline structure and phase composition of CS-GO, crucial for understanding its stability and structural integrity. Scanning electron microscopy (SEM) was utilized to examine the surface morphology of CS-GO, providing high-resolution images that depict particle size, shape, and surface characteristics. SEM analysis helps in evaluating the adsorbent's structural features and its potential interactions with contaminants in practical applications. Fourier-transform infrared spectroscopy (FTIR) conducted on a Perkin Elmer Spectrum Two identified the functional groups present on the surface of CS-GO. FTIR spectra indicate chemical bonds and molecular interactions, offering insights into the surface chemistry and potential binding sites available for adsorption processes. Dynamic light scattering (DLS) analysis using a Malvern ZSU1002 further characterized the average particle size distribution of CS-GO. This measurement is crucial for understanding the dispersion and stability of the adsorbent in aqueous solutions, providing valuable information for applications where particle size impacts performance. Together, these analytical techniques provided a comprehensive characterization of CS-GO, highlighting its optical, structural, morphological, chemical, and size-related properties.

2.2.5 Calibration Curve data analysis

CS-GO adsorbent performed a full-scale Ultraviolet Visible Spectroscopy scan. The outcome indicates that the adsorbent contains MB with measurements taken between 640 and 700 nm, MB exhibits its adsorbent peak at roughly 664 nm. UV-Vis Spectrophotometer was utilized to collect data for all batch study samples in this investigation. Therefore, it is verified by the UV analysis that the Methylene blue mixture removal percentage achieved by the CS-GO adsorbent is relevant and effective. The concentration vs absorbance data was plotted in the graph and an equation was Obtained corresponding to the curve, which follows Calibration Curve equation.

Calibration Curve is as follows

ABS OF MB DYE = 0.144 * CONCENTRATION OF MB DYE

R^2 of this Curve was MB for 0.99792 which is close to 1. This indicated data is closed to Trendline.

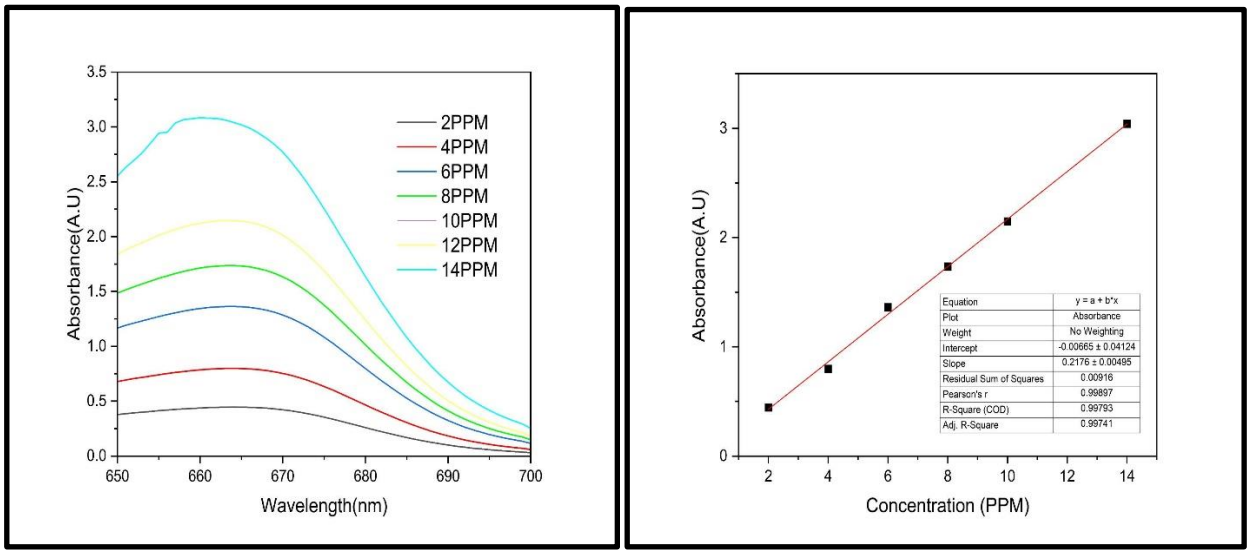


Fig 3A and 3B: Absorbance vs Wavelength graph & Absorbance vs Concentration graph.

2.2.6 Batch Study

In this Batch study the initial MB-dye concentration of 10–70 mg/L was employed. The pH of the MB-dye solution varied from 3 to 12. Various dosage of adsorbents (1-9 g/L). A temperature in the range of 35-75 ◦C was applied. After phase separation 0.1 mL of the stirring solution was diluted to 10.0 mL with distilled water and MB-dye concentrations were measured at 664 nm. The dye removal percentage(%R) is defined as

$$\%R=(C_0 - C_t)/C_0$$

where, Co and Ct are the initial concentrations and the final concentrations of dye at time t, respectively.

The other quantity is adsorption capacity. This quantity reveals the amount of adsorbent required to adsorb a particular amount of adsorbate (mg/g). The mathematical formula is,

$$Q_m = (C_0 - C_e)*V/m$$

Here, V is the volume of adsorbate aqueous solution (ml) and m is the mass of the adsorbent used in the batch adsorption process (mg).

CHAPTER- 3

RESULTS AND DISCUSSION

3.1 Characterization

3.1.1 Scanning Electron Microscope Micrograph

The SEM images depicted in the Figure illustrate the formation of semi-spherical gel beads using the dripping technique, where the CS-GO solution is introduced into a NaOH solution (Figure2). These beads exhibit a non-homogeneous surface structure with evenly distributed CS particles, contributing to increased surface roughness that enhances adsorption efficiency (Figure 4A and 4B) Upon initial reuse, observed changes in the SEM images reveal a reduction in the surface roughness of GO-CS beads. This smoothing effect is likely due to treatment with HCl, which desorbs previously adsorbed species from the bead surface. Subsequent regeneration cycles further demonstrate a trend towards a highly smooth surface texture (Fig 5A and 5B) These findings highlight the dynamic changes in surface morphology and texture of CS-GO beads during repeated use, influenced by desorption processes that affect their adsorption capacity and efficiency. Such observations are crucial for understanding the practical longevity and performance stability of these adsorbent materials in applications such as wastewater treatment and environmental remediation.

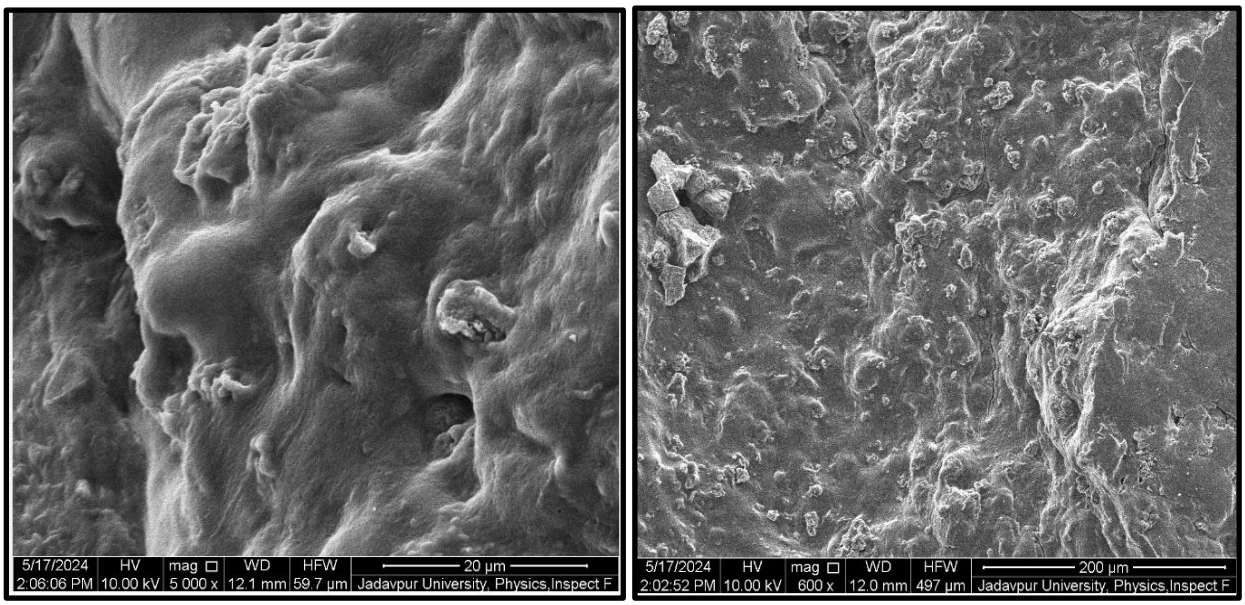


Fig 4A and 4B (The SEM images of CS-GO Beads untreated)

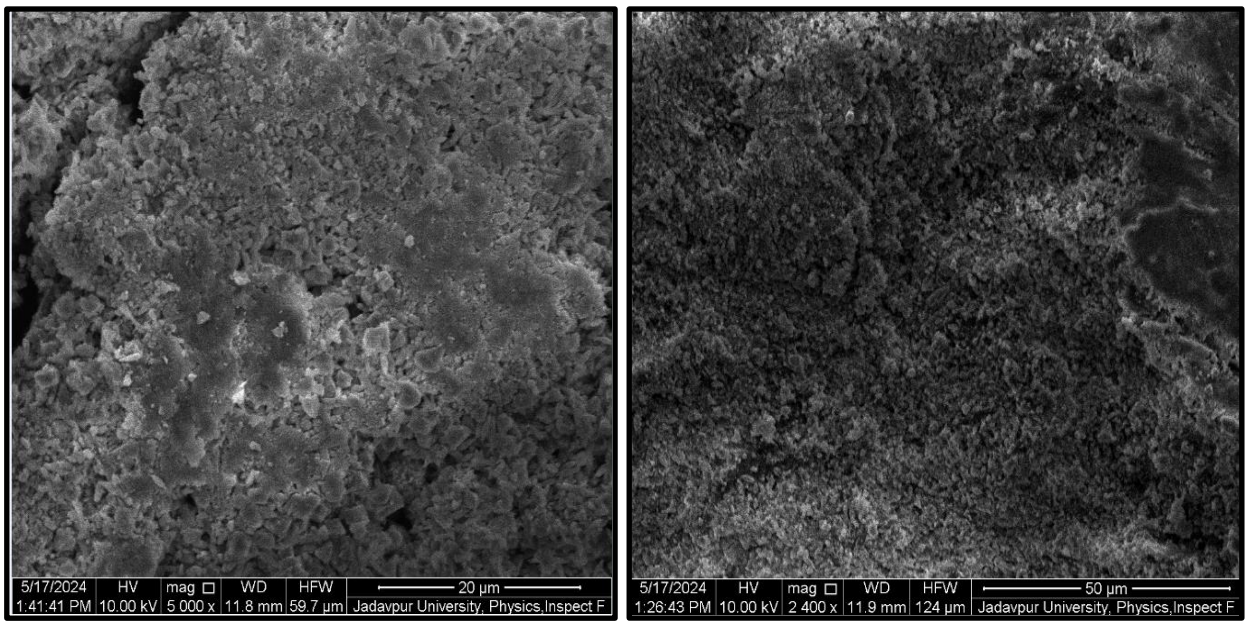


Fig 5A and 5B (The CS-GO Beads treated with MB)

3.1.2 X-Ray Diffraction Analysis

The structural properties of CS-GO and treated CS-GO-MB were investigated by X-ray diffraction (XRD) In the XRD pattern of (Fig.6) the peak was found at 2Θ = 19.78˚with a corresponding d-spacing of 4.434 Ǻ. The CS Exhibited a broad peak, due to the amorphous structure of the substance Upon formation of synthesized CS-GO beads making CS as a layer exhibited a diffraction peak at 2Θ= 21.52°, with a d-spacing of 0.061 Ǻ .There was a slight shift due to addition of GO thoroughly loaded with Chitosan. The results indicate that there are mainly physical interactions (hydrogen bonding) but not much of chemical reaction between CS and GO.

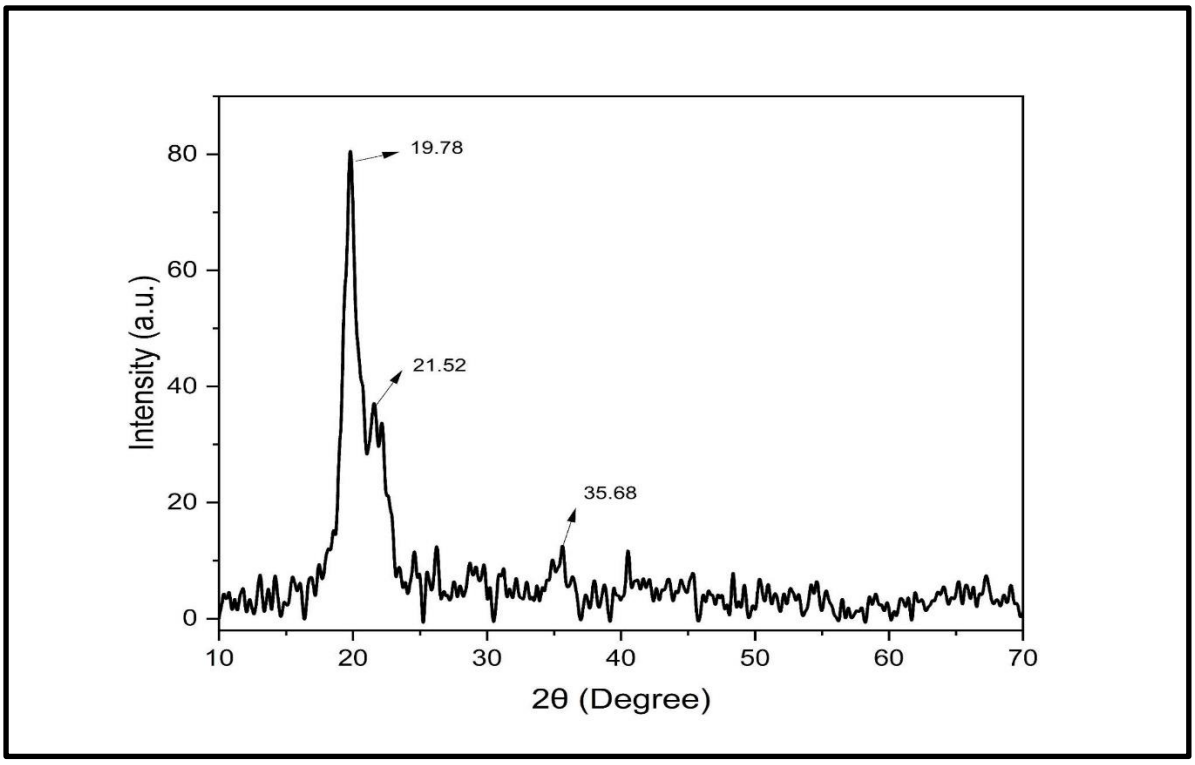


Fig 6: XRD patterns of CS-GO Beads.

Table 1: XRD Parameters:

Sample	**2θ**	**d-spacing(Ä)**
CS	19.78	4.434
GO	21.52	0.061

3.1.3 Fourier Transform Infrared Ray Analysis

FTIR spectroscopy is a powerful tool for identifying different functional groups in materials. Figure displays the FTIR spectra of GO, CS-GO, MB, and CS-GO-MB complexes. For GO, characteristic peaks appear at 2884 cm−1 (surface-adsorbed water), 1635 cm−1 (carboxylic group), 1588 cm−1 (water bending motion), 1377 cm−1 (carbonyl group deformation), and 1030 cm−1 (C-O bond stretching). The FTIR spectrum significantly changes when GO and CS are mixed to form beads, indicating successful integration of these materials. The CS-GO beads exhibit peaks at 1412 cm−1 (C-H stretching), 1082 cm−1 (water bending), and 1027 cm−1 (chitosan N-H bond Stretching) (Fig 7A). Upon adsorption of MB dye onto the CS-GO beads, the FTIR spectrum of the CS-GO-MB complex shows a red shift in peaks compared to the CS-GO spectrum, indicating successful MB dye adsorption. These spectral shifts confirm the interaction between MB dye and the functional groups on the CS-GO beads, demonstrating the beads' effective adsorption capacity (Fig 7B). This analysis highlights the structural and chemical changes occurring during the adsorption process, providing insights into the efficiency and mechanism of dye removal using CS-GO beads.

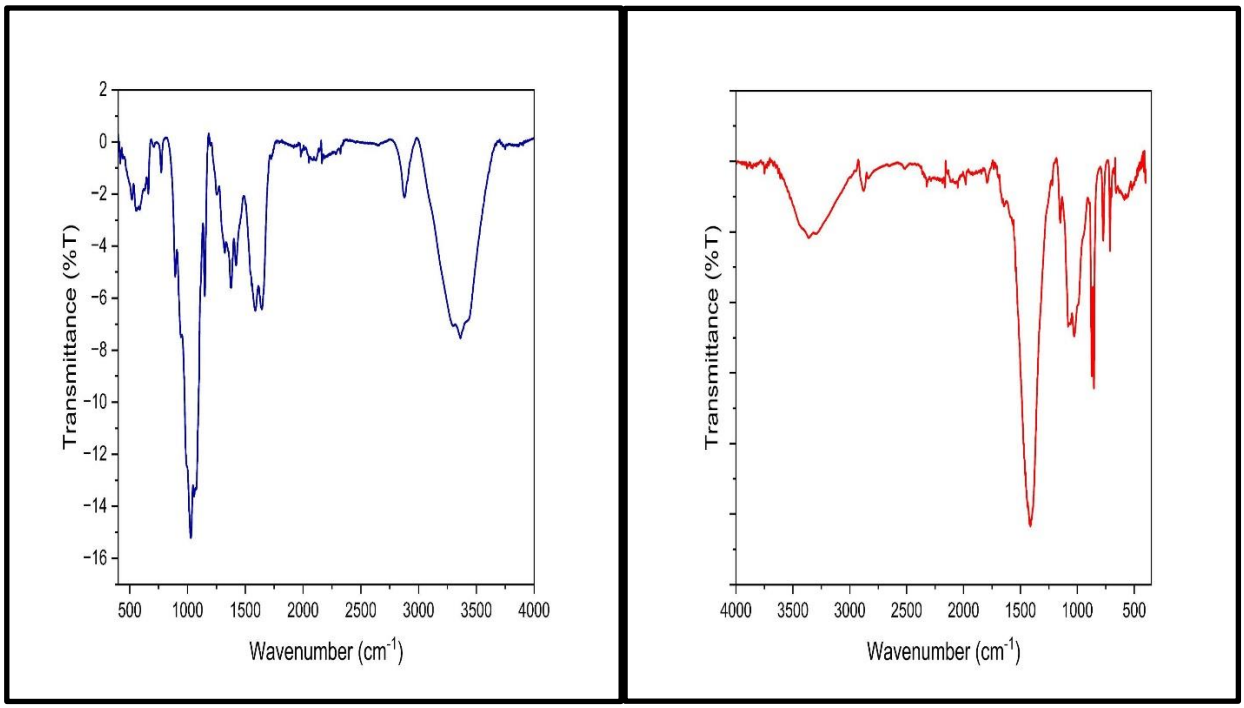


Fig7A and 7B: FTIR Patterns of CS-GO beads, MB treated CS-GO Beads.

3.1.4 DLS Analysis

Dynamic Light Scattering (DLS) is used to determine the size distribution profile of particles. The DLS of GO and CS-GO composite was shown in figure. It can be seen that synthesized adsorbent was in the size of 3130 nm for GO and 2330 nm for Synthesized CS-GO (Fig 8A and 8B) Z- average Values show a good correlation. Particle size deviation was observed and expected. This is caused due to agglomeration of CS-GO and GO influences both measurements.

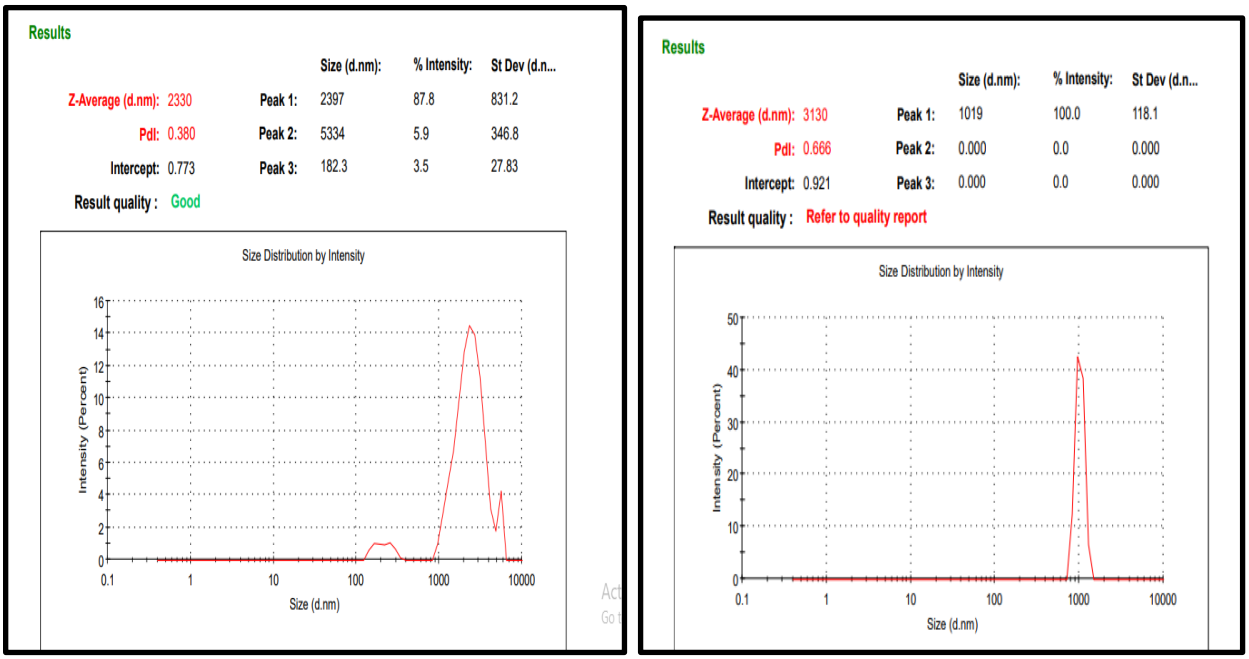


Fig 8A and 8B: DLS Analysis graphs of GO and GO-CS Beads.

.

3.1.5 Effect of Zero Point Discharge

To calculate ΔpH (pH_{f}--pH_{i}), the adsorption solution's final pH (pH_{f}) was evaluated. After that, the point of zero charge associated with the CS-GO was found by plotting a relation between ΔpH vs. pH_{i}, as shown in Figure 9.It was observed that point of the initial pH 7.83 as the point of zero discharge. Even though the adsorbent was situated in an extremely acidic environment, the graph demonstrated that it was negatively charged.

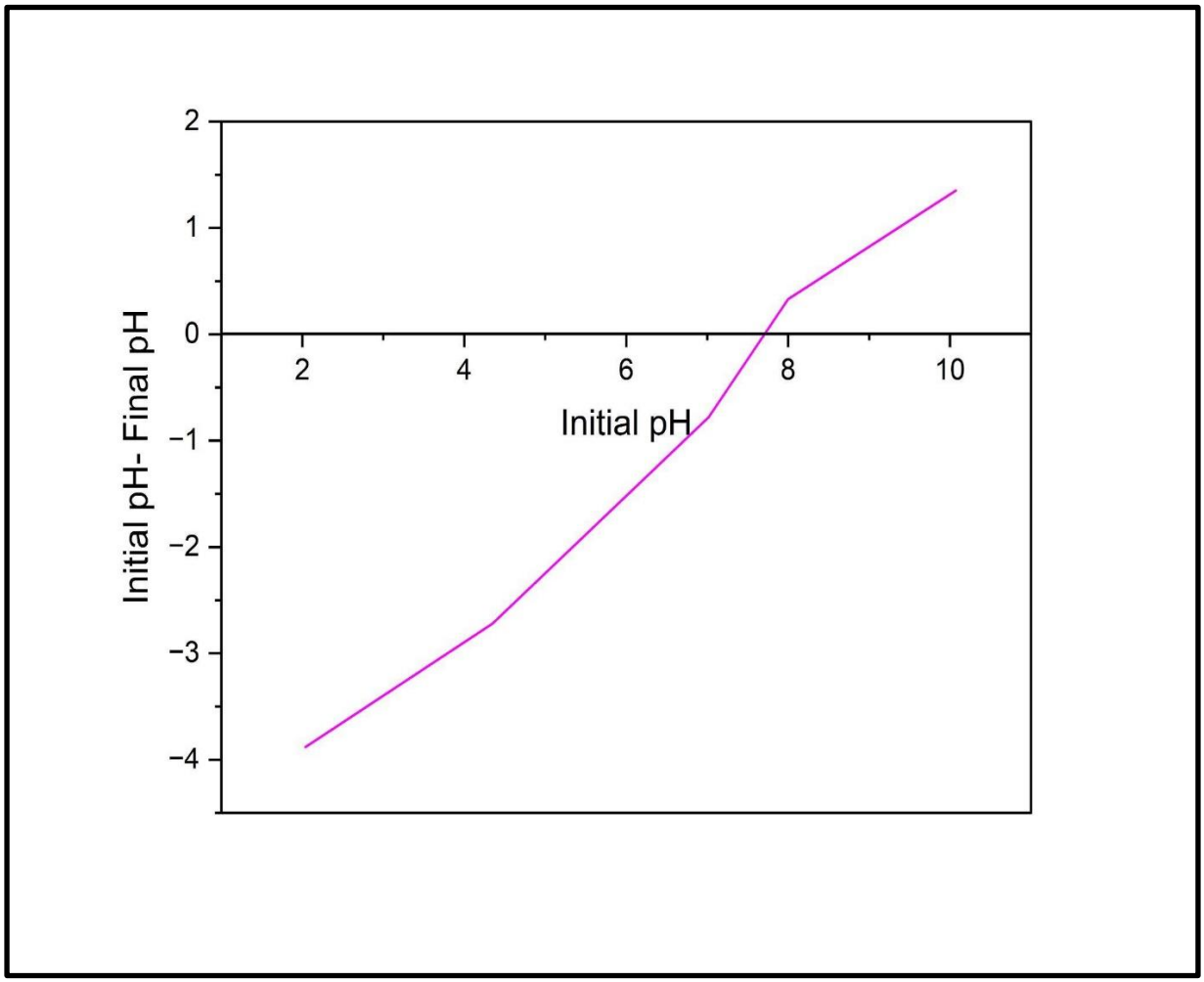


Fig9: Effect of Zero Discharge point on CS-GO beads.

4. Effects of Parameters

4.1 pH Study

An important characteristic to consider while researching adsorption processes is pH. The effect of pH was studied with initial Concentration of 30 PPM, and adsorbent dosage 5g/300ml, contact time was set for 24 hours and pH was varied in the range 3 to 12 & Stirring speed of 350 RPM. This is because the ionization of the binding sites for CS-GO composite beads is significantly impacted by the pH of the aqueous media. This study examined the impact of pH & increase in removal percentage of the starting solution on the adsorption effectiveness of MB dye in aqueous media, and the results are shown in Figure10. It is interesting to note that there is a linear increase in the adsorption capacity from 1.018 mg/g to 1.633 mg/g. when the pH of the solution rises in the range of (3–12). This is due to the binding site becoming protonated in an acidic environment, making it unsuitable for the adsorption of cationic MB-species A higher pH value (here pH 12) of the solution will result in a lower H+ concentration and more binding sites become increasingly ionized, creating a condition that is ideal for the effective removal of cationic MB-dye.

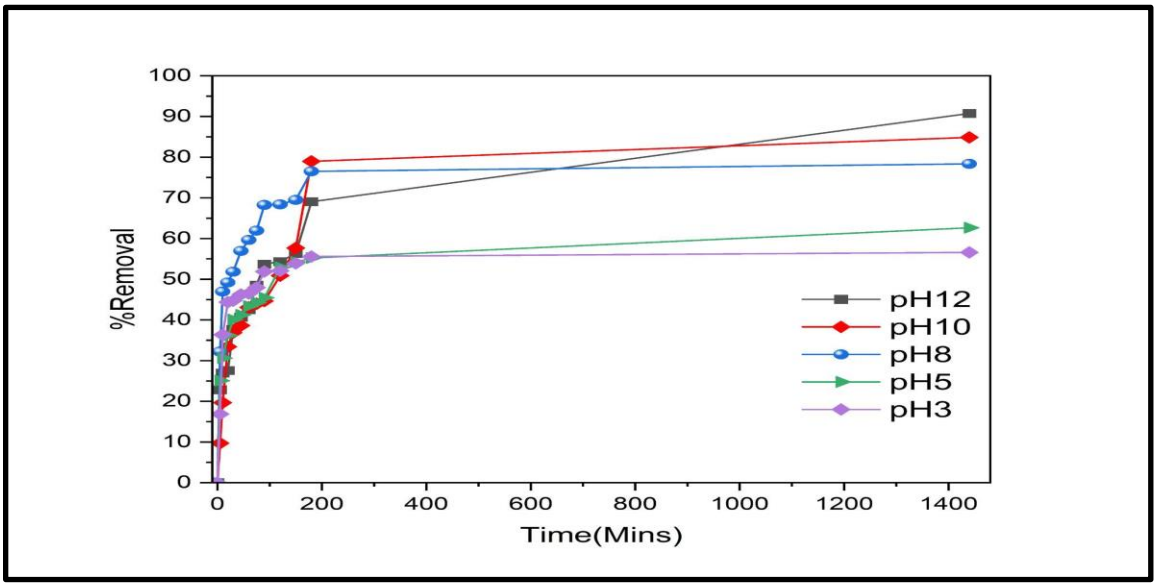


Fig10: Effect of Various pH study on Removal percentage.

4.2.2 Effect of Initial Concentration

Adsorption capacity and removal efficiency for the batch study was tested in initial MB Concentration of 10-70 PPM. As shown in Figure 11, the first induced MB-dye concentrations were tested in the range 10,30,50 and 70 PPM. The findings indicate that adsorption capacities of MB-dye concentrations were increased from 0.570 mg/g to 63.99 mg/ and the removal percentage ratio of MB over CS-GO beads decreased from 95 to 63%. This discovery is explained by the hypothesis that the number of MB-dye species will equal the number of binding sites on the surface of CS-GO beads at low MB dye concentrations. Reduced adsorption performance results from an increase in dye concentration because there are more dye species in the aqueous solution than there are binding sites.

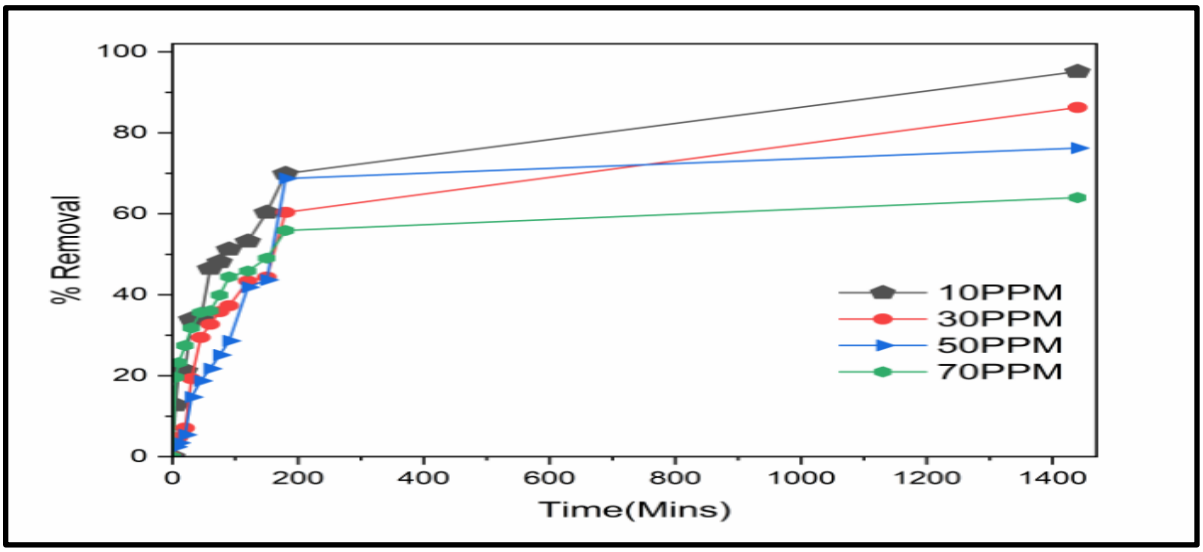


Fig11: Removal percentage on Effect of Various initial Concentration against Time.

4.2.3 Effect of Adsorbent Dosage

The effect of the adsorbent dose of CS-GO composite beads on the MB-dye removal efficiency is shown in Figure 12.It is observed that a higher dose of CS-GO composite beads improved the MB-dye's adsorption performance. It was observed that if Adsorbent Dosage was increased from 1g/L to 9g/L, the removal efficiency was increased from 48% to 91.8% after 24 hours, but the adsorption capacities decreased from 4.320 mg/g to 0.918 mg/g, while increasing of adsorbent dosage, as it offers various binding sites for fruitful interaction with additional MB-dye species.

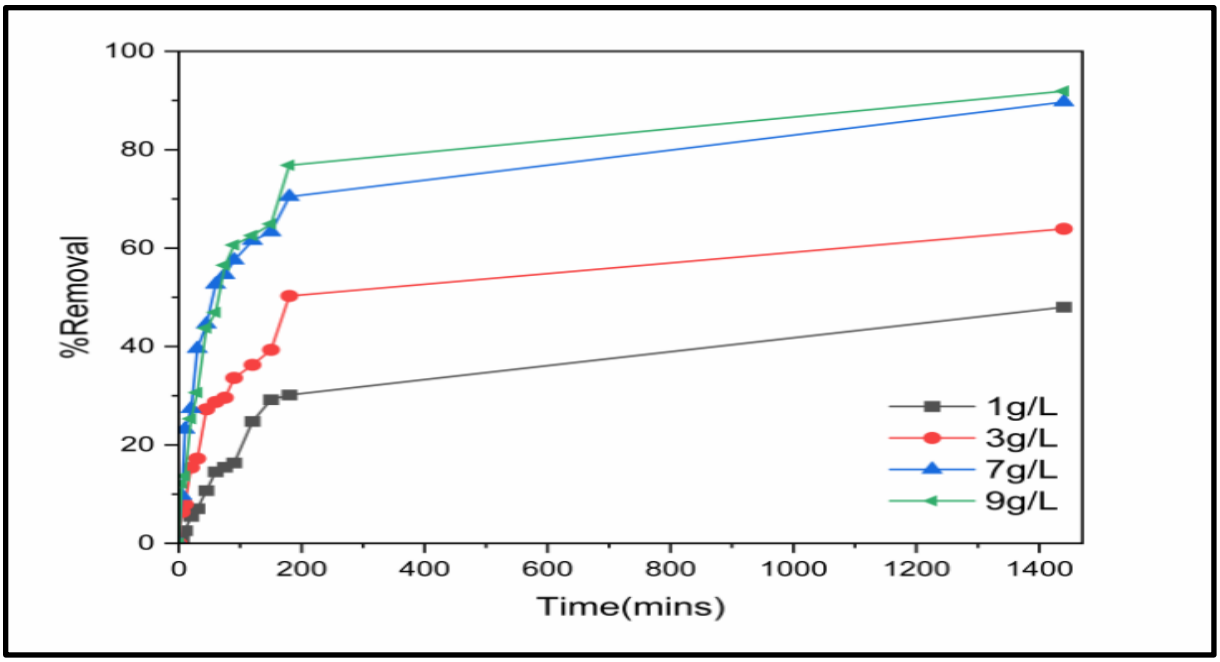


Fig12: Removal percentage on Effect of Adsorbent Dosage against Time.

4.2.4 Effect of Temperature

Effect of Temperature Shows a very slight influence on adsorption efficiency of MB-dye, as noted in figure 13 that further increase in temperature from 35℃ to 75℃, leads to decrease in removal percentage from 90% to 64 %, whereas the adsorption capacity increases from 1.40 mg/g to 10.80 mg/g. This indicated the adsorption process was an endothermic process. Although in room temperature (35℃) Shows the best removal of MB by CS-GO beads.

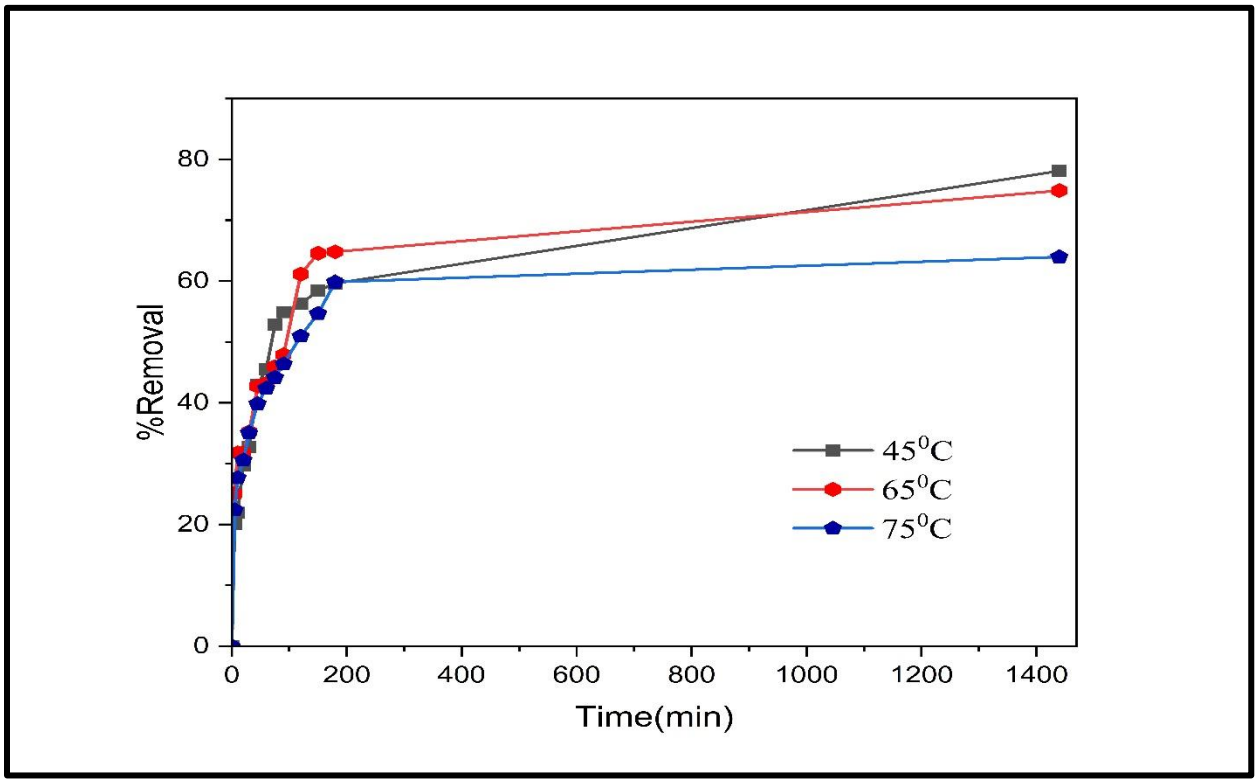


Fig13: Removal percentage on Effect of Various Temperature against Time.

4.3 ADSORPTION ISOTHERM

Adsorption isotherms describe how adsorbates interact with the adsorbents and how they are distributed between the liquid phase and the solid phase at equilibrium. These isotherms are crucial for understanding and designing adsorption processes. There are several models of adsorption isotherms, each with different assumptions and applications. Here are some of the most common types:

1. Langmuir Isotherm

The Langmuir isotherm assumes monolayer adsorption on a surface with a finite number of identical sites. This is the first proposed isotherm for gas adsorption on a solid, with assumptions such as adsorption occurring in a single layer, a fixed number of adsorptive sites, no steric hindrances between adsorbed molecules and the adsorbent surface, and no phase changes.

$$Q_{e=}Q_{max} \,.\, K_l C_e/(1+K_l.\, C_e)$$

Q_e: Amount of adsorbate adsorbed per unit weight of adsorbent at equilibrium (mg/g)

Q_{max} : Maximum adsorption capacity (mg/g)

K_l: Langmuir adsorption constant (L/mg)

C_e: Equilibrium concentration of adsorbate in the solution (mg/L)

We can Linearize the equation as:

$$Q_e/C_e = C_e/Q_{max} + 1/(\, Q_{max.}K_l)$$

Another important factor in this isotherm is the Separation Factor R_l The expression for R_l is as follows:

$R_l = 1 / (1+ K_l.\, C_0)$

where C_0 is the maximum initial concentration (mg/L). A value of R_l between 0 and 1 indicates a favorable adsorption process. The adsorption process is linear for (R_l = 1), unfavorable for (R_l > 1), and irreversible for (R_l = 0).

This empirical model assumes monolayer adsorption, meaning the adsorbed layer is one molecule thick, and adsorption can only occur at a finite (fixed) number of definite localized sites that are identical and equivalent. There is no lateral interaction or steric hindrance between the adsorbed molecules, even on adjacent sites. The Langmuir isotherm, which this model derives from, refers to homogeneous adsorption, where each molecule possesses constant enthalpies and sorption activation energy, with all sites having equal affinity for the adsorbate, and no transmigration of the adsorbate in the plane of the surface.

2. Freundlich Isotherm

The Freundlich isotherm is an empirical model that applies to adsorption on heterogeneous surfaces.

This model does not restrict adsorption to a monolayer and considers multilayer adsorption. The mathematical expression is as follows:

$$Log\ Q_e = Log\ K_f + \frac{1}{n} Log C_e$$

Here, K_f and n are isotherm constants that describe the adsorption capacity and adsorption intensity, respectively. The value of 1/n between 0 and 1 provides a quantitative measurement of the adsorption intensity, shifting to a less uniform distribution as the value approaches zero. A value larger than 1 indicates cooperative adsorption, while a value less than 1 suggests that a conventional Langmuir isotherm might explain the adsorption process without losing generality.

The linearized form of the isotherm equation is:

$$Ln\ Q_e = Ln\ K_f + \frac{1}{n} Ln\ C_e$$

The Freundlich isotherm is the earliest known relationship describing non-ideal and reversible adsorption, not limited to monolayer formation. This empirical model can be applied to multilayer adsorption, with a non-uniform distribution of adsorption heat and affinities over a heterogeneous surface. Currently, the Freundlich isotherm is widely applied in heterogeneous systems, especially for organic compounds or highly interactive species on activated carbon and molecular sieves.[50]

3. Temkin Isotherm

The Temkin isotherm considers the effects of indirect adsorbate/adsorbate interactions on adsorption isotherms. The isotherm includes a factor that explicitly accounts for adsorbent-adsorbate interactions. By disregarding extremely low and high concentration values, the model assumes that the heat of adsorption (a function of temperature) for all molecules in the layer decreases linearly with coverage rather than logarithmically.

$$Q_e = B_T.LnK_T + B_T.Ce$$

Q_e : Amount of adsorbate adsorbed per unit weight of adsorbent at equilibrium (mg/g)

K_T : Temkin isotherm constant (L/g)

B_T: Temkin constant related to adsorption heat (J/mol)

R: Universal gas constant (8.314 J/mol K)

T: Temperature (K)

The linear forms of the Langmuir, Freundlich, and Temkin isotherms, as well as the nonlinear forms of the Langmuir and Freundlich isotherms, were analyzed. Based on the R^2value, it was concluded that the Langmuir linear isotherm provided the best fit for this study. Similarly, for the nonlinear isotherms, the Langmuir isotherm was the best option to explain the process. Thus, the adsorption following the Langmuir isotherm (both linear and non-linear fit) suggests that the adsorption occurs through a monolayer mechanism.

Table 2: Linear Adsorption isotherm parameters

Model	Parameters	Values
Langmuir	K_l Q_{max} R_l R^2	0.33390 2.96832 0.041 0.99467
Freundlich	K_f n	1.755405 0.408525

	R^2	0.9853
Temkin	B_T K_T R^2	0.54008 5.39569 0.9922

Table 3: Non-Linear Adsorption parameters:

Model	**Parameters**	**Values**
Langmuir	Q_{max} K_l R^2 X^2	2.688 -2.053 -6.5587 2.505
Freundlich	K_f n R^2 X^2	0.91112 2.8824 0.9697 0.0261

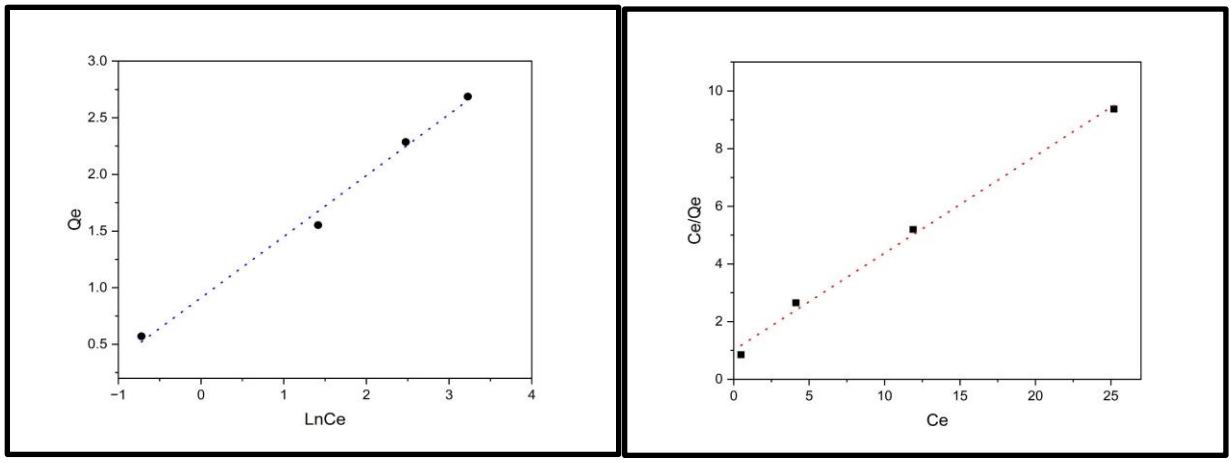
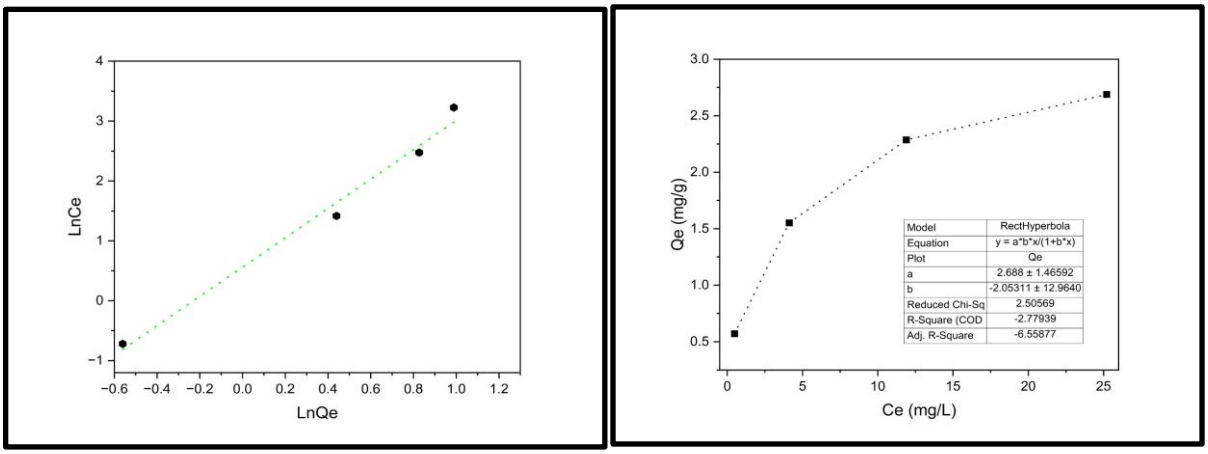


Fig14A & B: Linear Langmuir & Temkin isotherm Plot of MB



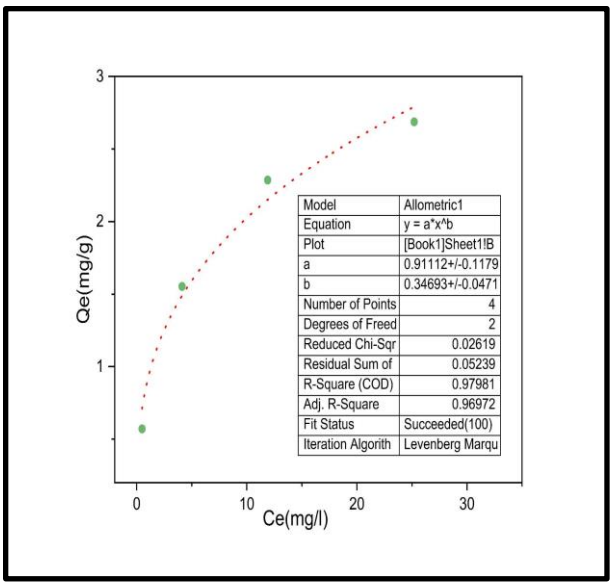


Fig 14C, D, E (Left to right)- Linear Freundlich, Non-Linear Langmuir and Non-Linear Freundlich plot of MB.

4.4 ADSORPTION KINETICS

Understanding the adsorption rate, mechanism, and effectiveness requires knowledge of adsorption kinetics. The design of an adsorption system must take into account the adsorption kinetics. pseudo-first-order, pseudo-second-order and Intra particle diffusion kinetics had been studied in this experiment.

Pseudo-first-order Kinetics: It assumes one of the reactants is at an abundant amount and so the change in the concentration is negligible. The linear form of this equation is given below,

$$Ln(Q_e - Q_t) = -K_1 . t + LnQ_e$$

Here, Q_e and Q_t are the adsorption capacity at equilibrium and at any time t respectively and K_1 is the kinetics constant

Pseudo-second-order Kinetics: The linearized form of kinetics equation is,

$$t/Q_t = t/Q_e + 1/K_2 . Q_e^2$$

Intra-particle Diffusion: The diffusion of adsorbate molecules can be studied by the intra-particle diffusion model.

$$Q_e = K_P t^{0.5}$$

K_P is the inter-particle diffusion rate constant ($mg.g^{-1}.min^{-0.5}$) which can be found from the Q_e vs $t^{0.5}$ plot.

Table4 : Adsorption Kinetics Data

Models	**Parameters**	**Values**
Pseudo-first order	K_1	0.00561
	Q_e	1.205832
	R^2	0.94007
Pseudo second order	K_2	1.266079
	Q_e	0.193695
	R^2	0.96125
Intra particle Diffusion	K_P	0.09652
	R^2	0.98048

Intra particle diffusion is dominant as it has a larger R^2 value and lesser error. So it can be stated that the process is following Intra particle diffusion kinetics. Following a Intra particle diffusion reaction means non-linearity is observed, multiple process are limiting overall adsorption rate favoring chemisorption over Physisorption.[56]

The intraparticle model's most appropriate.It is advised to do multiple tests in order to determine the best way to divide the adsorption kinetics data based on the statistical parameter values. The diffusion of the adsorbate in the adsorbent's pores is the mass transfer step that determines intraparticle diffusion model, rather than determining whether the model lines pass through (0, 0), the statistical parameters should be utilized to assess the fitting findings.[51]

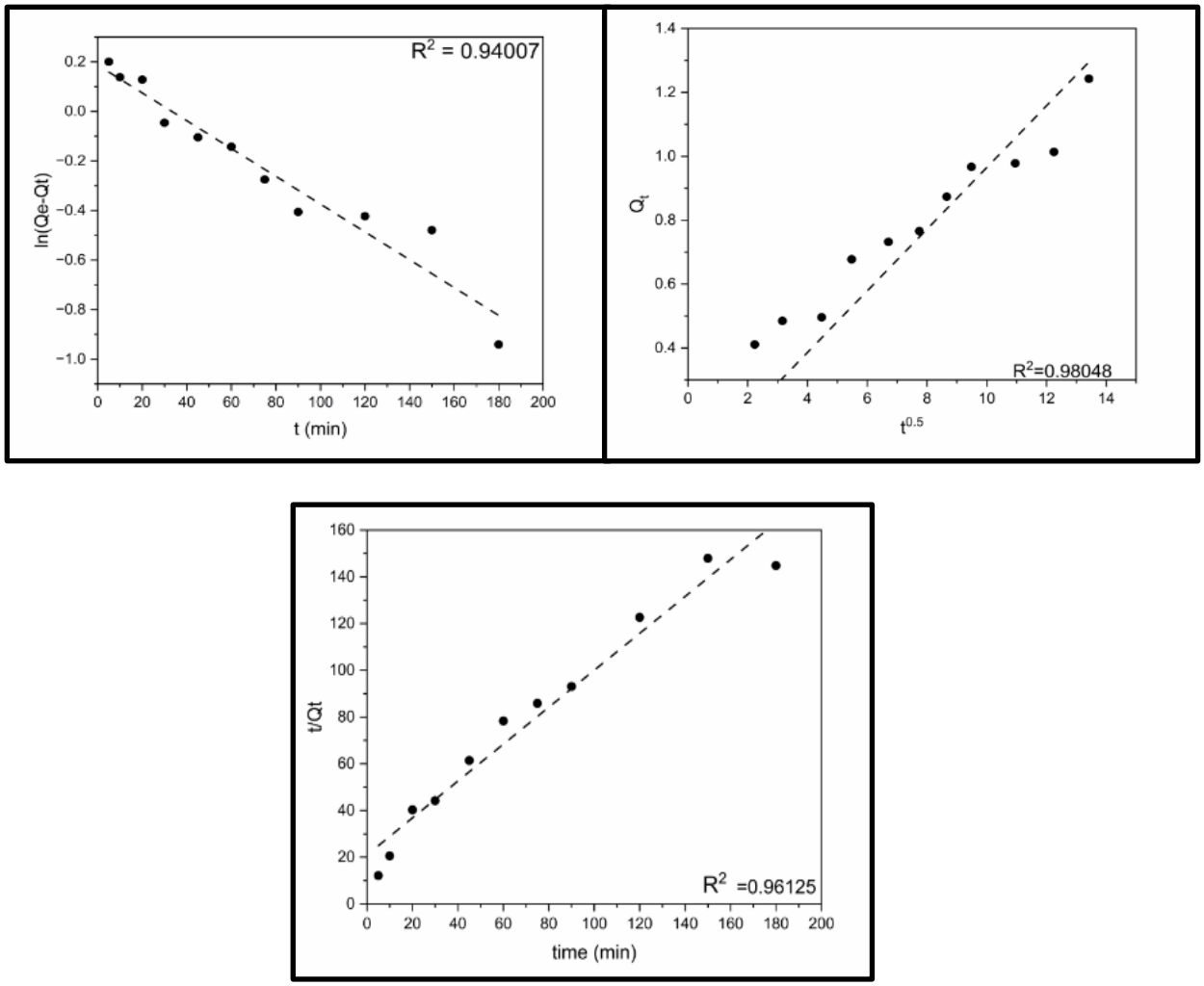


Fig 15A,B and C: (From Top to bottom) Pseudo First order, , Intra diffusion particle and Pseudo second order kinetics plot of MB dye over CS-GO beads.

4.5 ADSORPTION THERMODYNAMICS

Batch adsorption process were carried out at different temperatures(308,318,338,348 K) for thermodynamic batch study of the adsorption process. The results obtained from the conducting Batch experiments were used to find out various thermodynamic parameters like Gibbs's free Energy Change($\Delta G_{adsorption}$), change in enthalpy($\Delta H_{adsorption}$), change in entropy($\Delta S_{adsorption}$) and Thermodynamic equilibrium constant(K_c).Following equations are used in this study,

$$Ln\ K_c = \Delta S/R - \Delta H/RT$$

$$\Delta G = \Delta H - T\Delta S$$

$$K_c = Q_e/C_e$$

Here, Q_e and C_e are the equilibrium adsorption capacity(mg/g)and equilibrium Concentration of the adsorbate(PPM). R is the universal gas constant. (8.314 J/mol/K).

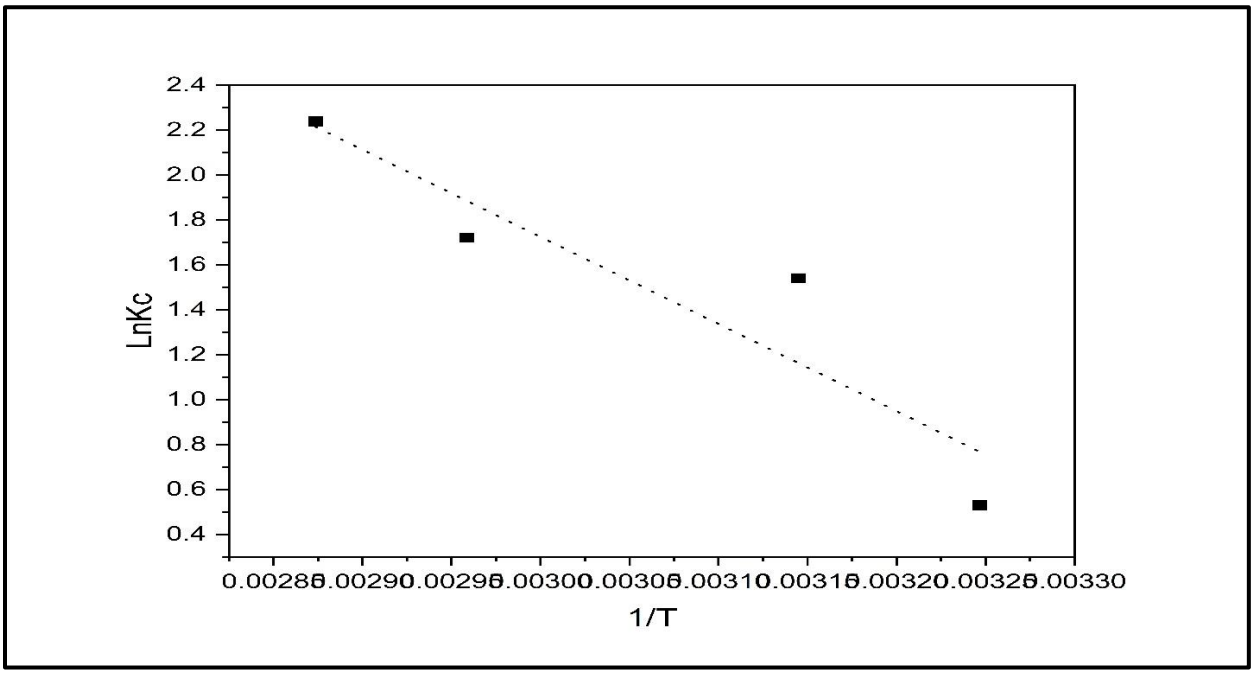


Fig 16. Thermodynamic Study of MB adsorption on CS-GO

Table 5: Adsorption Thermodynamics Data

Temp(K)	C_e(PPM)	Q_e(mg/g)	K_C	$\Delta G_{adsorption}$(J/mol)	$\Delta H_{adsorption}$ (J/mol)	$\Delta S_{adsorption}$ (J/mol)
308	2.778321	1.633301	1.701047	-1965.942	32255.05	111.107
318	6.565356	1.406079	4.669265	-3077.014		
338	7.536078	1.347835	5.591247	-5299.156		
348	10.8096	1.151424	9.388027	-6410.228		

We tend to observe that $\Delta H_{adsorption}$ Shows positive value as the temperature increases. This is due to temperature increase, the internal energy of system increases. Now we already know, enthalpy Change is directly proportional to internal energy change. That is why, $\Delta H_{adsorption}$ Shows positive results. As temperature increases, Kinetic energy of the system also increases. Higher Kinetic energy means higher randomness of the molecules in the system. So the $\Delta S_{adsorption}$ Show positive value. Negative Gibb's free energy in four different temperatures indicates that the Adsorption process is spontaneous. The spontaneity of the system increases with increase in Temperature.

4.6 REGENERATION STUDY

A regeneration study (Fig.17) was conducted to assess the economic viability of the adsorbent. Here the optimum adsorption conditions extracted from the batch investigation were observed to study the adsorbent recyclability. After each cycle, the adsorbent was washed with a (10ml,0.1%) solution of HCl. The adsorbent was then neutralized by washing with distilled water until pH7 and dried in a hot air oven at 60°C for 1 hour. The initial MB concentration was set at 30 ppm, and the adsorbent dosage was 5g. The removal efficiency decreased from 83% to 31% after four cycles of batch adsorption, the removal efficiency declined at the end of 3 cycles. Therefore, it can be concluded that by blocking some binding sites by highly interacted dye species leading to occupying these binding sites and making them unavailable for further adsorption.

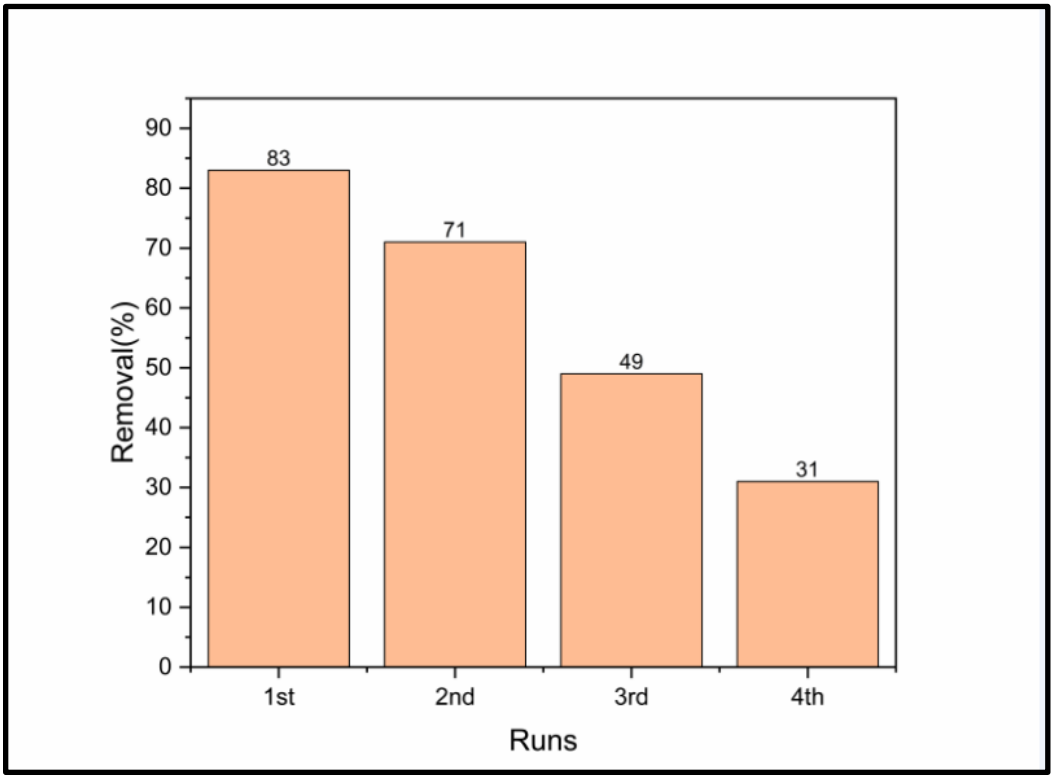


Figure17: Regeneration Study of MB Adsorption on CS-GO.

4.7 COMPARISON STUDY TABLE OF VARIOUS ADSORBENT OF PREVIOUS WORK WITH THE PRESENT WORK.

Adsorbent	**Maximum Adsorption Capacity(mg/g)**	**Isotherm Model**	**Kinetics Model**	**References**
Graphene oxide Chitosan Composite	402.6 mg/g	Langmuir	Pseudo- Second Order	[38]
Silk-Fibroin Graphene Oxide	381.67 mg/g	Freundlich	Pseudo- Second Order	[35]
Polydopamine microspheres	90.07 mg/g	Langmuir	Pseudo- Second Order	[26]
Didodecyl dimethyl ammonium bromide Brown clay	164 mg/g	Langmuir	Pseudo- Second Order	[25]
Graphene oxide	714 mg/g	Langmuir	Not studied	[47]
H2SO4 cross-linked magnetic chitosan beads	20.408 mg/g	Langmuir	Pseudo- Second Order	[37]
Pine cone biomass(*pinus radiata)*	109.89 mg/g	Langmuir	Pseudo- Second Order	[48]
Chitosan based	1599.03 mg/g	Langmuir	Pseudo- Second Order	[23]

Porous carbon microspheres				
Wheat shells	21.50 mg/g	Langmuir	Pseudo- Second Order	[49]
Chitosan Graphene oxide Hydrogel	23.26 mg/g	Langmuir	Pseudo Second order	[36]
Graphene	153.85 mg/g	Langmuir	Pseudo second order	[53]
Fly Ash	0.0014 mg/g	Freundlich	Not studied	[54]
Perlite	7.118 mg/g	Langmuir	Not studied	[55]
Chitosan Graphene oxide Beads	1.633 mg/g	Langmuir	Intra particle Diffusion	This work

CHAPTER 4:

CONCLUSION

5.1 Conclusion

In order to adsorb the dye Methylene blue (MB) from wastewater, this group Chitosan Functionalized Graphene-Oxide (CS-GO) composite beads formed using continuous dropping procedures. SEM, DLS, FTIR, and XRD were among the methods used to characterize the manufactured (CS-GO) composite beads in order to look into their chemical and physical characteristics. The greatest absorption capacity under ideal circumstances was 1.633 mg g−1. Graphite flakes were converted into graphene oxide using a modified version of Hummer's Method. Next, a 6 (M) NaOH solution is used to decrease the graphene oxide. To characterize the adsorbent, the SEM, XRD, FTIR, and DLS analyses were performed. The SEM data demonstrates that MB dye layer was successfully deposited on the Chitosan graphene oxide beads by observing the roughness. The greater diffraction peak was observed due to presence of Chitosan along with Graphene Oxide has been detected with the use of XRD data. The FTIR data demonstrates that when about the functional groups present in CS-GO, CS-GO MB. According to a pH analysis, the highest elimination efficiency has been reached at pH 12. The influence of initial adsorbate concentration demonstrates that the removal efficiency falls with increasing initial MB concentration for a given amount of adsorbent. However, in the case of adsorbent dose, removal efficiency increases if we increase the adsorbent dosage for a fixed quantity of starting MB concentration. However, as time went on, the active sites were being occupied, which caused the rate of adsorption to decline. The process reached the equilibrium stage after a whole day. Kinetic analysis was conducted. regarding pseudo-second- and pseudo-first-order kinetics and intra particle diffusion. In comparison to pseudo-first-order kinetics, pseudo-second-order kinetics, intra particle diffusion model exhibits a larger value and a smaller error. Thus, it can be said that IPD(Intra particle diffusion) have been followed by the process. Langmuir Freundlich and Temkin isotherm was examined in the isotherm study. Examined were both linear and nonlinear fits. The Langmuir isotherm, which has a maximum adsorption capacity and best fit, exhibits superior performance in both linear and nonlinear fit. Up to four batch adsorption cycles were conducted for the regeneration investigation. The removal rate decreased to 31% from 83%. Therefore, the adsorbent of CS-GO beads can be washed by the 1% HClsolution.

REFERENCES:

[1] Sokolowska-Gajda. Synthetic dyes based on environmental considerations. Dye Pigment 1996;30(1):1–20. https://doi.org/10.1016/0143-7208(95)00048-8

[2] Ivanov K. Possibilities of using zeolite as a filler and carrier for dyestuffs in paper. Papier-Zeitschrift fur die Erzeugung von Holzstoff Zellstoff Papier und Pappe 1996;50(7):456–9.

[3] Kabdaşli I, Tünay O, Orhon D. Wastewater control and management in a leather tanning district. Water Sci Technol 1996;40(1):261–7. https://doi.org/10.1016/0273-1223(99)00393-8

[4] Bensalah N, Alfaro M, Martínez-Huitle C. Electrochemical treatment of synthetic wastewaters containing Alphazurine A dye. Chem Eng J 2009;149(1):348–52.https://doi.org/10.1016/j.cej.2008.11.031

[5] Wróbel D, Boguta A, Ion RM. Mixtures of synthetic organic dyes in a photoelectrochemical cell. J Photochem Photobiol A Chem 2001;138(1):7–22. https://doi.org/10.1016/S1010-6030(00)00378-0

[6] Nath, J., Chowdhury, A., & Dolui, S. K. (2018). Chitosan/graphene oxide-based multifunctional pH-responsive hydrogel with significant mechanical strength, self-healing property, and shape memory effect. *Advances in Polymer Technology*, *37*(8), 3665–3679. https://doi.org/10.1002/adv.22151.

[7] Field MS, et al. An assessment of the potential adverse properties of fluorescent tracer dyes used for groundwater tracing. Environ Monit Assess 1995;38(1):75–96. https://doi.org/10.1007/BF00546786

[8] He LM, Tebo BM. Surface charge properties of and Cu (II) adsorption by spores of the marine Bacillus sp. strain SG-1. Appl Environ Microbiol 1998;64(3):1123–9. https://doi.org/10.1128/AEM.64.3.1123-1129.1998

[9] Yagub, M. T., Sen, T. K., Afroze, S., & Ang, H. M. (2014). Dye and its removal from

aqueous solution by adsorption: A review. In *Advances in Colloid and Interface Science* (Vol. 209, pp. 172–184). Elsevier. https://doi.org/10.1016/j.cis.2014.04.002

[10] Hsu TC, Chiang CS. Activated sludge treatment of dispersed dye factory wastewater. J Environ Sci Health A 1997;32(7):1921–32. https://doi.org/10.1080/10934529709376655

[11] Wong Y, et al. Adsorption of acid dyes on chitosan—equilibrium isotherm analyses. Process Biochem 2004;39(6):695–704. https://doi.org/10.1016/S0032-9592(03)00152-3

[12] Sen TK, Afroze S, Ang H. Equilibrium, kinetics and mechanism of removal of methylene blue from aqueous solution by adsorption onto pine cone biomass of Pinus radiata. Water Air Soil Pollut 2011;218:499–515. https://doi.org/10.1007/s11270-010-0531-2

[13] Yagub MT, Sen TK, Ang H. Equilibrium, kinetics, and thermodynamics of methylene blue adsorption by pine tree leaves. Water Air Soil Pollut 2012;223(8):5267–82. https://doi.org10.1007/s11270-012-1214-7

[14]Sabzevari, M., Cree, D. E., & Wilson, L. D. (2018). Graphene Oxide-Chitosan Composite Material for Treatment of a Model Dye Effluent. *ACS Omega*, *3*(10), 13045–13054. https://doi.org/10.1021/acsomega.8b01871

[15] Khandegar, V., Kaur, P. J., & Chanana, P. (2021). Chitosan and graphene oxide-based nanocomposites for water purification and medical applications: a review. *BioResources*, *16*(4), 8525.

[16]Zhuang, S., & Wang, J. (2019). Removal of cobalt ion from aqueous solution using magnetic graphene oxide/chitosan composite. *Environmental Progress and Sustainable Energy*, *38*(s1), S32–S41. https://doi.org/10.1002/ep.12912

[17]Abd-Elhamid, A. I., Aly, H. F., Soliman, H. A. M., & El-Shanshory, A. A. (2018). Graphene oxide: Follow the oxidation mechanism and its application in water treatment. *Journal of Molecular Liquids*, *265*, 226–237. https://doi.org/10.1016/j.molliq.2018.05.127

[18]Al-Fawwaz, A. T., & Abdullah, M. (2016). Decolorization of Methylene Blue and Malachite Green by Immobilized Desmodesmus sp. Isolated from North Jordan. *International Journal of*

Environmental Science and Development, *7*(2), 95–99. https://doi.org/10.7763/IJESD.2016.V7.748

[19]Almeida, C. A. P., Debacher, N. A., Downs, A. J., Cottet, L., & Mello, C. A. D. (2009). Removal of methylene blue from colored effluents by adsorption on montmorillonite clay. *Journal of Colloid and Interface Science*, *332*(1), 46–53. https://doi.org/10.1016/j.jcis.2008.12.012

[20]ALSamman, M. M., & Sánchez, J. (2022). Chitosan- and Alginate-Based Hydrogels for the Adsorption of Anionic and Cationic Dyes from Water. *Polymers*, *14*(8). https://doi.org/10.3390/polym14081498

[21]Arunachalam, K. D. (2021). Bio-adsorption of methylene blue dye using chitosan-extracted from Fenneropenaeus indicus shrimp shell waste. *Journal of Aquaculture & Marine Biology*, *10*(4), 146–150. https://doi.org/10.15406/jamb.2021.10.00316

[22]Atun, G., Hisarli, G., Sheldrick, W. S., & Muhler, M. (2003). Adsorptive removal of methylene blue from colored effluents on fuller's earth. *Journal of Colloid and Interface Science*, *261*(1), 32–39. https://doi.org/10.1016/S0021-9797(03)00059-6

[23]Deng, W., Tang, S., Zhou, X., Liu, Y., Liu, S., & Luo, J. (2020). Honeycomb-like structure-tunable chitosan-based porous carbon microspheres for methylene blue efficient removal. *Carbohydrate Polymers*, *247*. https://doi.org/10.1016/j.carbpol.2020.116736

[24]Dindorkar, S. S., Patel, R. V., & Yadav, A. (2022). Adsorptive removal of methylene blue dye from aqueous streams using photocatalytic CuBTC/ZnO chitosan composites. *Water Science and Technology*, *85*(9), 2748–2760. https://doi.org/10.2166/wst.2022.142

[25]*Effective Adsorptive Removal of Methylene Blue from Water by Didodecyldimethylammonium Bromide-Modified Brown Clay*. (n.d.)

[26]Fu, J., Chen, Z., Wang, M., Liu, S., Zhang, J., Zhang, J., Han, R., & Xu, Q. (2015). Adsorption of methylene blue by a high-efficiency adsorbent (polydopamine microspheres): Kinetics, isotherm, thermodynamics and mechanism analysis. *Chemical Engineering Journal*, *259*, 53–61. https://doi.org/10.1016/j.cej.2014.07.101

[27]Ghaedi, M., Nazari, E., Sahraie, R., & Purkait, M. K. (2014). Kinetic and isotherm study of Bromothymol Blue and Methylene blue removal using Au-NP loaded on activated carbon. *Desalination and Water Treatment*, *52*(28–30), 5504–5512. https://doi.org/10.1080/19443994.2013.822156

[28]Ghosh, D., & Bhattacharyya, K. G. (n.d.). *Adsorption of methylene blue on kaolinite*. www.elsevier.com/locate/clay

[29]Gunathilake, B. M., Jayawardana, D., Pupulewatte, P. G. H., Dissanayake, S., & Manage, P. M. (2023). Removal of methylene blue from aqueous solution using raw laterite: An adsorption study. *Journal of the National Science Foundation of Sri Lanka*, *51*(1), 53–67. https://doi.org/10.4038/jnsfsr.v51i1.10886

[30]Gürses, A., Doğar, Ç., Yalçin, M., Açikyildiz, M., Bayrak, R., & Karaca, S. (2006). The adsorption kinetics of the cationic dye, methylene blue, onto clay. *Journal of Hazardous Materials*, *131*(1–3), 217–228. https://doi.org/10.1016/j.jhazmat.2005.09.036

[31]Li, Y., Du, Q., Liu, T., Peng, X., Wang, J., Sun, J., Wang, Y., Wu, S., Wang, Z., Xia, Y., & Xia, L. (2013). Comparative study of methylene blue dye adsorption onto activated carbon, graphene oxide, and carbon nanotubes. *Chemical Engineering Research and Design*, *91*(2), 361–368. https://doi.org/10.1016/j.cherd.2012.07.007

[32]Liu, H., Sun, R., Feng, S., Wang, D., & Liu, H. (2019). Rapid synthesis of a silsesquioxane-based disulfide-linked polymer for selective removal of cationic dyes from aqueous solutions. *Chemical Engineering Journal*, *359*, 436–445. https://doi.org/10.1016/j.cej.2018.11.148

[33]Liu, Q., Yu, H., Zeng, F., Li, X., Sun, J., Li, C., Lin, H., & Su, Z. (2021). HKUST-1 modified ultrastability cellulose/chitosan composite aerogel for highly efficient removal of methylene blue. *Carbohydrate Polymers*, *255*. https://doi.org/10.1016/j.carbpol.2020.117402

[34]Marotta, A., Luzzi, E., De Luna, M. S., Aprea, P., Ambrogi, V., & Filippone, G. (2021). Chitosan/zeolite composite aerogels for a fast and effective removal of both anionic and cationic dyes from water. *Polymers*, *13*(11). https://doi.org/10.3390/polym13111691

[35]Martis, L. J., Parushuram, N., & Sangappa, Y. (2022). Preparation, characterization, and methylene blue dye adsorption study of silk fibroin–graphene oxide nanocomposites. *Environmental Science: Advances*, *1*(3), 285–296. https://doi.org/10.1039/d1va00047k

[36]Nayl, A. E. A. A., Abd-Elhamid, A. I., Arafa, W. A. A., Ahmed, I. M., El-Shanshory, A. A., Abu-Saied, M. A., Soliman, H. M. A., Abdelgawad, M. A., Ali, H. M., & Bräse, S. (2022). Chitosan-Functionalized-Graphene Oxide (GO@CS) Beads as an Effective Adsorbent to Remove Cationic Dye from Wastewater. *Polymers*, *14*(19). https://doi.org/10.3390/polym14194236

[37]Rahmi, Ismaturrahmi, & Mustafa, I. (2019). Methylene blue removal from water using H2SO4 crosslinked magnetic chitosan nanocomposite beads. *Microchemical Journal*, *144*, 397–402. https://doi.org/10.1016/j.microc.2018.09.032

[38]Sabzevari, M., Cree, D. E., & Wilson, L. D. (2018). Graphene Oxide-Chitosan Composite Material for Treatment of a Model Dye Effluent. *ACS Omega*, *3*(10), 13045–13054. https://doi.org/10.1021/acsomega.8b01871

[39]Sakib, M. N., Hano, N., Takafuji, M., & Ahmed, S. (2022). Preparation of chitosan/laterite/iron oxide-based biocomposite and its application as a potential adsorbent for the removal of methylene blue from aqueous solution. *Environmental Nanotechnology, Monitoring and Management*, *17*. https://doi.org/10.1016/j.enmm.2022.100658

[40]Taofeek Popoola, L. (2019). Characterization and adsorptive behaviour of snail shell-rice husk (SS-RH) calcined particles (CPs) towards cationic dye. *Heliyon*, *5*, 1153. https://doi.org/10.1016/j.heliyon.2019

[41]Van Hoa, N., Minh, N. C., Cuong, H. N., Dat, P. A., Nam, P. V., Viet, P. H. T., Phuong, P. T. D., & Trung, T. S. (2021). Highly porous hydroxyapatite/graphene oxide/chitosan beads as an efficient adsorbent for dyes and heavy metal ions removal. *Molecules*, *26*(20). https://doi.org/10.3390/molecules26206127

[42]Wang, R., Yu, Q., He, Y., Bai, J., Jiao, T., Zhang, L., Bai, Z., Zhou, J., & Peng, Q. (2019). Self-assembled polyelectrolyte-based composite hydrogels with enhanced stretchable

and adsorption performances. *Journal of Molecular Liquids*, *294*. https://doi.org/10.1016/j.molliq.2019.111576

[43]Wang, Z., Zhang, G., & Li, Y. (2020). Preparation of chitosan/polyacrylamide/graphene oxide composite membranes and study of their methylene blue adsorption properties. *Materials*, *13*(19), 1–18. https://doi.org/10.3390/ma13194407

[44] Siregar, P.M.S.B.N; Lesbani, A;(2016) Mg_Al chitosan as a selective adsorbent in removal of Methylene Blue from Aqueous Solutions. https://doi.org/10.26554/sti.2022.7.2.170-178

[45] A.I. Abd-Elhamid, H.F. Aly, Hesham A.M. Soliman, Ahmed A. El-Shanshory,Graphene oxide: Follow the oxidation mechanism and its application in water treatment,Journal of Molecular Liquids,Volume 265,2018,Pages226-237,ISSN0167-7322, https://doi.org/10.1016/j.molliq.2018.05.127.

[46]Abd-Elhamid,A.I;Doma,A.S;Eco-friendly activation of charcoal for purification of water from colored organic pollutants March 2019 Research Journal of Chemistry and Environment 23(3):83-9523(3):83-95

[47]Yang, S. T., Chen, S., Chang, Y., Cao, A., Liu, Y., & Wang, H. (2011). Removal of methylene blue from aqueous solution by graphene oxide. *Journal of Colloid and Interface Science*, *359*(1), 24–29. https://doi.org/10.1016/j.jcis.2011.02.064

[48]Sen, T. K., Afroze, S., & Ang, H. M. (2011). Equilibrium, kinetics and mechanism of removal of methylene blue from aqueous solution by adsorption onto pine cone biomass of Pinus radiata. *Water, Air, and Soil Pollution*, *218*(1–4), 499–515. https://doi.org/10.1007/s11270-010-0663-y

[49]Bulut, Y., & Aydin, H. (2006). A kinetics and thermodynamics study of methylene blue adsorption on wheat shells. *Desalination*, *194*(1–3), 259–267. https://doi.org/10.1016/j.desal.2005.10.032

[50]Foo, K. Y., & Hameed, B. H. (2010). Insights into the modeling of adsorption isotherm systems. In *Chemical Engineering Journal* (Vol. 156, Issue 1, pp. 2–10). https://doi.org/10.1016/j.cej.2009.09.013

[51]Revellame, E. D., Fortela, D. L., Sharp, W., Hernandez, R., & Zappi, M. E. (2020). Adsorption kinetic modeling using pseudo-first order and pseudo-second order rate laws: A review. In *Cleaner Engineering and Technology* (Vol. 1). Elsevier Ltd. https://doi.org/10.1016/j.clet.2020.100032

[52]Isotherm Studies of Methylene Blue Adsorption onto Potassium Salts-Modified Textile Sludge - Scientific Figure on ResearchGate. Available from: https://www.researchgate.net/figure/Molecular-structure-of-methylene-blue_fig1_281738079 [accessed 23 Jul 2024]

[53]Liu, T., Li, Y., Du, Q., Sun, J., Jiao, Y., Yang, G., Wang, Z., Xia, Y., Zhang, W., Wang, K., Zhu, H., & Wu, D. (2012). Adsorption of methylene blue from aqueous solution by graphene. Colloids and Surfaces B: Biointerfaces, 90(1), 197–203. https://doi.org/10.1016/j.colsurfb.2011.10.019

[54] Mohan, D., Singh, K. P., Singh, G., & Kumar, K. (2002). *Removal of Dyes from Wastewater Using Flyash, a Low-Cost Adsorbent †*. https://doi.org/10.1021/ie010667

[55] Do, M., Gan, ˇ, Alkan, M., & Onganer, Y. (2000). *ADSORPTION OF METHYLENE BLUE FROM AQUEOUS SOLUTION ONTO PERLITE*.

[56] Sahoo, T. R., & Prelot, B. (2020). Adsorption processes for the removal of contaminants from wastewater: The perspective role of nanomaterials and nanotechnology. In *Nanomaterials for the Detection and Removal of Wastewater Pollutants* (pp. 161–222). Elsevier. https://doi.org/10.1016/B978-0-12-818489-9.00007-4

[57] Queiroz, M. F., Melo, K. R. T., Sabry, D. A., Sassaki, G. L., & Rocha, H. A. O. (2015). Does the use of chitosan contribute to oxalate kidney stone formation? *Marine Drugs*, *13*(1), 141–158. https://doi.org/10.3390/md13010141

[58]Banerjee, P., Barman, S. R., Mukhopadhayay, A., & Das, P. (2017). Ultrasound assisted mixed azo dye adsorption by chitosan–graphene oxide nanocomposite. *Chemical Engineering Research and Design*, *117*, 43–56. https://doi.org/10.1016/j.cherd.2016.10.009